The LINNEAN SOCIETY of London BIOLOGICAL Journal of the Linnean Society

Biological Journal of the Linnean Society, 2015, **116**, 834–846. With 4 figures.

Microevolutionary patterns in the common caiman predict macroevolutionary trends across extant crocodilians

KENICHI W. OKAMOTO[1,2*,†], R. BRIAN LANGERHANS[3], REZOANA RASHID[1,4] and PRIYANGA AMARASEKARE[1]

[1]*Department of Ecology and Evolutionary Biology, University of California, Los Angeles, Los Angeles, CA, 90095, USA*
[2]*Department of Entomology, North Carolina State University, Raleigh, NC, 27695, USA*
[3]*Department of Biological Sciences and W.M. Keck Center for Behavioral Biology, North Carolina State University, Raleigh, NC, 27695, USA*
[4]*USC School of Pharmacy, University of Southern California, Los Angeles, CA, 90089, USA*
[†]*Current address: Yale Institute for Biospheric Studies, Yale University, New Haven, CT, 06511, USA*

Received 29 May 2015; revised 28 June 2015; accepted for publication 28 June 2015

Both extinct and extant crocodilians have repeatedly diversified in skull shape along a continuum, from narrow-snouted to broad-snouted phenotypes. These patterns occur with striking regularity, although it is currently unknown whether these trends also apply to microevolutionary divergence during population differentiation or the early stages of speciation. Assessing patterns of intraspecific variation within a single taxon can potentially provide insight into the processes of macroevolutionary differentiation. For example, high levels of intraspecific variation along a narrow-broad axis would be consistent with the view that cranial shapes can show predictable patterns of differentiation on relatively short timescales, and potentially scale up to explain broader macroevolutionary patterns. In the present study, we use geometric morphometric methods to characterize intraspecific cranial shape variation among groups within a single, widely distributed clade, *Caiman crocodilus*. We show that *C. crocodilus* skulls vary along a narrow/broad-snouted continuum, with different subspecies strongly clustered at distinct ends of the continuum. We quantitatively compare these microevolutionary trends with patterns of diversity at macroevolutionary scales (among all extant crocodilians). We find that morphological differences among the subspecies of *C. crocodilus* parallel the patterns of morphological differentiation across extant crocodilians, with the primary axes of morphological diversity being highly correlated across the two scales. We find intraspecific cranial shape variation within *C. crocodilus* to span variation characterized by more than half of living species. We show the main axis of intraspecific phenotypic variation to align with the principal direction of macroevolutionary diversification in crocodilian cranial shape, suggesting that mechanisms of microevolutionary divergence within species may also explain broader patterns of diversification at higher taxonomic levels. © 2015 The Linnean Society of London, *Biological Journal of the Linnean Society*, 2015, **116**, 834–846.

ADDITIONAL KEYWORDS: adaptive radiation – *Caiman crocodilus* – geometric morphometrics – intraspecific variation – skull shape.

INTRODUCTION

Adaptive diversification within many crown groups exhibits repeated diversification of one or a few key traits (Rüber, Verheyen & Meyer, 1999; Moczek, 2006; Saxer, Doebeli & Travisano, 2010; Monnet, De Baets & Klug, 2011), as reviewed previously (Smith & Skulason, 1996; Schluter, 2000a; Glor, 2010; Elmer & Meyer, 2011). Explaining why such patterns of diversification persistently arise at the macroevolutionary scale remains a central challenge of evolutionary biology. Clarifying the mechanisms

*Corresponding author. E-mail: kenichi.okamoto@yale.edu

giving rise to these patterns requires an understanding of how processes driving microevolutionary divergence (changes within and among populations) can also generate macroevolutionary differentiation (Darwin, 1859; Dobzhansky, 1937; Simpson, 1944; Stanley, 1979; Gould, 2002). Linking patterns of diversification at these different scales requires testing parallelism with respect to (1) patterns of phenotypic diversification within species or during the early stages of speciation and (2) patterns of phenotypic diversification among broader groups of distantly-related species. If microevolutionary patterns of trait variation parallel macroevolutionary patterns of diversification, this suggests processes responsible for microevolutionary change over relatively short timescales may also generate broad patterns over longer timescales.

Crocodyliforms, including both extant and extinct lineages, exhibit consistent patterns of cranial shape diversity (Brochu, 2001; Pierce, Angielczyk & Rayfield, 2008; Piras *et al.*, 2009; Pearcy & Wijtten, 2011). For example, extant crocodilians include both brevirostrine, broad-snouted forms (e.g. *Caiman latirostris*) and longirostrine, narrow-snouted species (e.g. *Gavialis gangeticus*). Some of the more dramatic differences in cranial shape are found among different families, although even the single genus *Crocodylus* includes both narrow- and broad-snouted forms apparently evolving multiple times in different geographical regions (e.g. narrow-snouted species such as *Crocodylus johnsoni* in northern Australia and broad-snouted species such as *Crocodylus moreletti* in the Neotropics and *Crocodylus palustris* in south Asia; Oaks, 2011). Fossil crocodyliforms exhibit similar trends in cranial shape diversity. For example, deposits from the Middle Eocene across the Northern Hemisphere contain several species from distinct, geographically widespread groups (including planocraniid, tomistomine, gavialoid, and alligatorine specimens) whose crania range from short- to long-snouted morphs (Brochu, 2001). Although the fossil record from the Neogene in continents in the Southern Hemisphere (South America, Australia, and Africa) consists largely of endemic clades, cranial morphological diversity among crocodilians is still conspicuous in those regions as well (Brochu, 2003; Scheyer *et al.*, 2013). Despite differences in endemicity, the major morphological forms are represented in crocodyliforms from all three continents. Indeed, consistent diversification in cranial shapes appears to have occurred quite frequently. For example, after the Eocene, cranial shapes characterized by narrow snouts may have evolved independently on at least four occasions (Brochu, 1997).

Although the mechanisms underlying patterns of cranial shape diversity across crocodilians remain an active area of research (Sadleir & Makovicky, 2008; in addition to the studies noted above), patterns of cranial shape diversity within species are much less well-understood (Ayarzagüena, 1984; Hall & Portier, 1994). Clarifying the nature and extent of intraspecific variation in cranial morphology can be important for interpreting patterns of variation at higher taxonomic levels (Darwin, 1859; Schluter, 1996; Arnold, Pfrender & Jones, 2001; Calsbeek, Smith & Bardeleben, 2007). For example, the processes generating diversity across crocodilians may require macroevolutionary timescales to generate prevailing patterns of morphological diversity (Gingerich, 2001; Uyeda *et al.*, 2011). Alternatively, such diversity could have largely evolved within species over relatively shorter, microevolutionary timescales during population differentiation, with additional morphological divergence occuring over macroevolutionary timescales further accentuating phenotypic differences (Kinnison & Hendry, 2001). A comparative analysis of morphological variation within and between species of a lineage provides a way to determine whether major morphological diversification can occur on microevolutionary time scales. If intraspecific patterns of diversity parallel variation found between species or genera, this suggests that the same processes might be responsible for patterns of diversity at both scales, with macroevolutionary patterns reflecting an amplification of microevolutionary trends.

In the present study, we seek to clarify patterns of intraspecific variation in cranial morphology in an extant, widely distributed and abundant Neotropical species, the common caiman *Caiman crocodilus*. Geometric morphometrics (Bookstein, 1997) provides a systematic, robust, and quantitative framework for characterizing morphological diversity in crocodyliform cranial shapes (Busbey, 1997; Pierce *et al.*, 2008; Piras *et al.*, 2009; Pearcy & Wijtten, 2011). We apply this framework to assess cranial shape variation within the *C. crocodilus*/*Caiman yacare* complex, and compare intraspecific cranial shape diversity with interspecific cranial shape diversity among extant crocodilians. We discuss factors that may explain observed patterns of intraspecific variation, and evaluate the implications of observed patterns of intraspecific cranial shape variation within the context of cranial shape diversity across the Crocodylia more broadly.

MATERIAL AND METHODS

SPECIMENS

We examined cranial shape variation within the *C. crocodilus*/*C. yacare* complex because of their widespread geographical distribution across Central

and South America, apparent recent and ongoing diversification (two possible species, with four described subspecies), and availability of museum specimens (King & Burke, 1989; Busack & Pandya, 2001; Venegas-Anaya *et al.*, 2008). Although *C. crocodilus* and *C. yacare* are often regarded as separate species (Ross, 1998; Busack & Pandya, 2001), there may be some degree of introgression between the two groups. Using both mitochondrial and nuclear genes, Hrbek *et al.* (2008) found considerable haplotypic diversity within *C. crocodilus*, with the *C. yacare* haplotypes in their analysis nested within common *C. crocodilus* haplotypes. We therefore conducted our analysis for the *C. crocodilus*/*C. yacare* taxonomic complex. Performing analyses with only the four subspecies of *C. crocodilus* (i.e. excluding *C. yacare*) produces extremely similar results, as reported here, and does not affect any of our conclusions (see Supporting information, Data S1).

We examined 62 *Caiman crocodilus* and 31 *Caiman yacare* specimens, spanning the latitudinal range of the taxa (see Supporting information, Data S2). We only examined adult and subadult individuals because earlier work indicated that *Caiman* skull shape exhibits ontogenetic variation that could confound our analysis (Monteiro & Soares, 1997). Our analyses were therefore restricted to skulls with a total cranial length > 15 cm, a size that excluded skulls from hatchlings and very young juveniles (mean ± SD = 24.4 ± 4.4 cm, maximum cranial length = 34.2 cm). We further restricted our investigation to specimens collected from the wild (excluded those from captive settings) within the native range of the species. For *C. crocodilus*, we examined 47 specimens from museum collections and 15 specimens based on illustrations of the dorsal view of the cranium in Medem (1983), including all four putative subspecies (*Caiman crocodilus apaporiensis*, $N = 16$; *Caiman crocodilus chiapasius*, $N = 3$; *Caiman crocodilus crocodilus*, $N = 27$; and *Caiman crocodilus fuscus*, $N = 16$). The illustrations in Medem (1983) include information on the distance from the posterior tip of the supraoccipital to the anterior tip of the premaxillae contact for each specimen, permitting us to accurately scale the depictions. Specimens were classified into distinct subspecies based on accompanying specimen records. Although knowledge of the geographic ranges of most subspecies and major clades within *C. crocodilus* is becoming increasingly better characterized through molecular studies (Venegas-Anaya *et al.*, 2008), the cranial specimens used in the present study could only be assigned to different groups with near certainty if further molecular analyses on the specimens were to be performed. All *C. yacare* specimens examined were housed in museum collections.

Morphometrics

Snout shape for each specimen was characterized using geometric morphometrics, which seeks to provide a robust characterization of the geometric association between anatomical points (landmarks) (Rohlf & Marcus, 1993). We base our analysis on morphometric landmarks on the dorsal crania (Fig. 1) established in Pearcy & Wijtten (2011); these landmarks quantify and characterize snout shape variation across extant crocodilian species, and reliably distinguish between the brevirostrine, broad-snouted, and longirostrine, narrow-snouted, groups at higher taxonomic levels (Pearcy & Wijtten, 2011). However, we omitted two landmarks whose definitions rely on anatomical structures further removed from the homologous locus; in particular, the centres of the left and right orbits (landmarks 8 and 9; Pearcy & Wijtten, 2011). To avoid inflating the degrees of freedom, we used only a single set of the bilaterally symmetric landmarks in Pearcy & Wijtten (2011) for our analyses. The crania were photographed in the dorsal aspect with the sagittal plane aligning as perpendicularly as possible to a fixed camera's lens, and no noteworthy distortions were discerned across images. All landmarks were digitized using TPSDIG, version 2 (Rohlf, 2005).

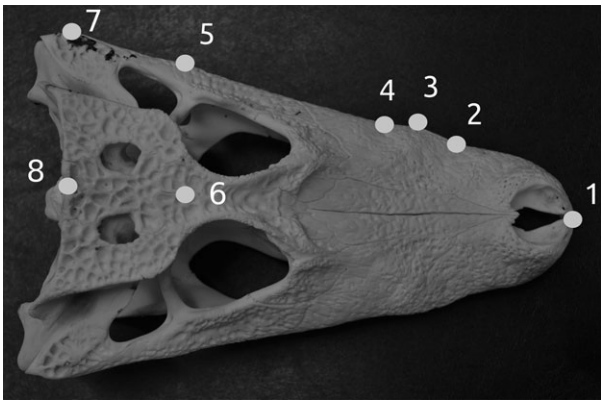

Figure 1. Landmarks used in the analysis, adapted from Pearcy & Wijtten (2011). (1) Anterior tip of the premaxillae contact. (2) Left side of the minimum width immediately posterior to the premaxilla–maxilla contact and anterior to the maximum preorbital width. (3) Left side of the maximum preorbital width posterior to the premaxilla–maxilla contact. (4) Left side of the minimum preorbital width posterior to the maximum preorbital width. (5) Left side of the skull at the posterior point of the orbital bar. (6) Midline of the width of the skull measured at the posterior point of the postorbital bar. (7) Left side of the maximum width of the quadratojugal bone. (8) Posterior tip of the supraoccipital.

Statistical analysis

The digitized landmarks were rotated, translated and scaled to standardize the coordinates using a generalized Procrustes analysis (GPA) in the geomorph and shapes packages in R (Dryden, 2012; Adams & Otárola-Castillo, 2013), thereby removing the effects of location, scale, and orientation from the raw landmark data. We used principal components (PC) derived from the standardized landmarks (i.e. relative warps) to quantify cranial shape variation among specimens.

Our basic approach to analyzing patterns of shape variation within the *C. crocodilus*/*C. yacare* complex was as follows. First, we characterized the contributions of different biological factors (allometry, taxonomic group within the *C. crocodilus*/*C. yacare* complex) to variation in the shape variables (relative warps). Second, we identified the primary morphological gradient of shape differences, controlling for allometric variation, within this complex, and projected individual specimens along this gradient. To facilitate interpretation of the morphological gradient, the underlying landmark coordinates were regressed against the projected scores, and the resulting predicted landmark coordinates were visualized using thin-plate splines. Third, we performed an analogous analysis on a dataset describing interspecific cranial shape variation, and projected allometrically-corrected average cranial shapes for the different subspecies in the *C. crocodilus*/*C. yacare* complex along the interspecifically-derived gradient of morphological variation. Finally, we tested whether the interspecific morphological gradient and the intraspecific morphological gradients parallel each other. Below, we describe this analysis in further detail.

Morphological differences among the five taxonomic groups were assessed by conducting a multivariate analysis of covariance (MANCOVA) and visualizing morphological differences using thin-plate spline transformation grids. For purposes of visualization, the landmarks with bilaterally symmetric counterparts were reflected about the sagittal plane in our thin-plate spline transformation grids.

The MANCOVA involved regressing all relative warps on the explanatory variables of taxonomic group, skull size, and their interaction. The statistical significance of each MANCOVA term was determined using an F-test based on Wilks's λ. We quantified the relative importance of model terms using Wilks's partial η^2 (Langerhans & DeWitt, 2004).

Terms for sex and approximate life stage were also evaluated. However, controlling for the effects of allometry, we found the effects of these factors on shape to be nonsignificant (see Supporting information, Data S3) and therefore removed them from the final analyses. Consequently, our analyses at the microevolutionary scale are based on MANCOVAs describing how the geometric shape variables varied according to size and taxonomic grouping. This allows us to assess the significance, relative magnitude, and nature of morphological differences among taxonomic groups at the same time as controlling for allometry:

$$\begin{aligned}\text{Relative warps} = {} & \text{Constant} + \text{Skull Size} \\ & + \text{Taxonomic group} + \text{Skull Size} \\ & \times \text{Taxonomic group} + \text{Error}\end{aligned}$$

The effects of skull size on cranial shape represent a reasonable measure of allometry because skull size is closely correlated with total body size in crocodilians (Webb & Messel, 1978; Hall & Portier, 1994; Verdade, 1999; Wu *et al.*, 2006; Platt *et al.*, 2009). We used the centroid size of the specimens (i.e. the square root of the sum of squared distances between landmarks and their centroid: the point defined by the dimension-wise means of the landmark's coordinates; Bookstein, 1997) to measure skull size. Centroid size was highly correlated with cranial length in our data-set ($r = 0.99$). We used analysis of variance to examine centroid size differences among taxonomic groups, and found no differences across taxa with considerable overlap in centroid size among all five taxonomic groups.

The allometric trend across taxonomic groups was visualized by regressing the shape variables (relative warps) on centroid size, and plotting the resulting shape scores against size (Drake & Klingenberg, 2008). The shape scores were calculated by projecting the shape variables (i.e. relative warps) onto a vector describing the linear effects of centroid size on each shape variable (Drake & Klingenberg, 2008). The landmark coordinates were then regressed against these shape scores and the predicted landmark coordinates of the largest and smallest individuals were visualized with thin-plate-spline deformation grids to illustrate how allometric trends affect skull shape.

Skull shape variation across taxa, independent of allometry, was evaluated by calculating morphological divergence vectors associated with the taxonomic group term of the model, following Langerhans & Makowicz (2009). The divergence vectors characterize the linear effect of the taxonomic group term of the MANCOVA on the multivariate shape variables (i.e. relative warps), controlling for the effects of cranial size (i.e. allometry: Langerhans, 2009; Langerhans & Makowicz, 2009; Franssen, 2011; Firmat *et al.*, 2012; Franssen, Stewart & Schaefer, 2013). As in Langerhans (2009), we used a broken-stick model (MacArthur, 1957; Frontier, 1976; Jackson, 1993; Legendre & Legendre, 1998) to identify which

divergence vectors accounted for a statistically significant share of the variation in cranial shape.

Differences in cranial shape among taxonomic groups were visualized using thin-plate spline regression of the major divergence vectors calculated from the MANCOVA. We used the key divergence vectors, which explained more variation than under the broken-stick tests for our visualizations. Individuals were projected onto the divergence vectors, and linear models were fit for predicting the landmark coordinates for each individual from their divergence vector score. The predicted landmark coordinates were then reflected about the saggital plane and mapped along with deformation grids relative to the mean predicted shape. Visualization of divergence vectors illustrated the major axes of phenotypic variation controlling for allometry among the closely-related taxonomic groups, with the goal of illustrating patterns of early cranial differentiation.

Finally, although highly detailed geographical data were generally unavailable, all *C. crocodilus* specimens were identifiable to the first level administrative districts (e.g. provinces and states) of the countries in which they were collected. The distribution of cranial shapes within *C. crocodilus* along the major divergence vectors among these geographical regions is shown in the Supporting information (Fig. S1).

Comparing intraspecific with interspecific variation

To compare microevolutionary patterns of cranial divergence among groups within the *C. crocodilus*/*C. yacare* complex with the macroevolutionary patterns of cranial divergence among crocodilians, we extracted mean Procrustes-transformed landmark data for 21 extant crocodilian species (all species except *C. crocodilus* and *C. yacare*) from Pearcy & Wijtten (2011) and examined patterns of cranial diversification at this taxonomic scale.

To examine major axes of cranial shape variation among species at the same time as controlling for allometry, we required estimates of mean cranial size for all extant crocodilian species. Although Pearcy & Wijtten (2011) do not specify the cranial sizes of their specimens, they do provide estimates of the relative mean cranial size for each species. Although it is unclear whether these relative sizes derive from the mean centroid sizes or another measure of cranial size, the relative mean cranial sizes illustrated in Pearcy & Wijtten (2011) presumably provide a reasonable estimate of each species' mean cranial size. Thus, we reconstructed relative cranial length from the depiction of mean relative cranial size in Pearcy & Wijtten (2011). We then rescaled the Procrustes-transformed mean landmark coordinates for each species by setting the Euclidean distance from the anterior tip of the premaxillae contact (landmark 1) to the posterior tip of the supraoccipital (landmark 13) equal to the relative cranial length for each species. The relative positions of the landmarks to each other remain unaffected by this rescaling. Centroid size for each species' average cranial shape was then calculated based on the rescaled landmarks.

To compare major axes of cranial shape variation across intraspecific and interspecific scales, we first characterized cranial shape for each data point using common units across these two taxonomic scales. We conducted a GPA to obtain all relative warps from the pooled dataset of 21 mean landmark coordinates from the interspecific data and landmark coordinates from 93 specimens in the *C. crocodilus*/*C. yacare* complex. These relative warps were retained as shape variables in the separate intra- and interspecific analyses described below,providing a one-to-one correspondence between the shape variables and the landmark coordinates for the specimens. Because our relative warps simply provide geometric shape variables in common units across the two taxonomic datasets with appropriate degrees of freedom as a result of GPA, and the divergence vectors are derived independently for the inter- and intraspecific datasets (see below), differences in the relative number of data points for each taxonomic scale do not bias the subsequent analyses. We conducted a multivariate regression of relative warps on centroid size separately for each taxonomic scale (interspecific and intraspecific), and retained the residual shape variables (i.e. relative warp scores) that constitute a 'size-free' estimate of cranial shape for each species/taxonomic group. For the intraspecific dataset, we then calculated the mean residual 'size-free' relative warp score for each subspecies in the the *C. crocodilus*/*C. yacare* complex. Our resulting residuals represent the average cranial shape for each species/taxonomic group, controlling for the effects of cranial size. We then conducted a PCA of the mean residuals separately for the interspecific and intraspecific taxa to derive the main vectors of morphological divergence for both groups. For the interspecific dataset, the first and second PCs (see Supporting information Fig. S2) explained a higher proportion of cranial morphological diversity than expected under a broken-stick model. For the intraspecifc groups, only the first PC explained more cranial morphological variation than the broken-stick model. Because only the first PC explained a statistically significant share of shape differences across both datasets, we used the first PC to characterize the principal axis Z_{macro} of morphological variability at the interspecific level (accounting for

approximately 53% of shape variance) and the intraspecific level (Z_{micro}; accounting for approximately 83% of shape variance). Although this procedure for deriving the intraspecific axis of variation differs slightly from the approach described above using MANCOVAs, this method was performed to render the analyses of intraspecific data comparable to the analyses of the interspecific data. Nevertheless, the resulting 'size-free' intraspecific axes of divergence from the two analyses were extremely similar (for group means, $r^2 = 0.99$), indicating that both approaches capture the same gradient in intraspecific variation.

To examine the similarity among the primary axis of phenotypic variability within species (microevolutionary variation) and among species (macroevolutionary variation), we calculated the angle between Z_{macro} and Z_{micro} (Klingenberg C, 1996). When the angle between two vectors equals 90°, there is no vector correlation between intra- and interspecific vectors. By contrast, a significantly smaller angle between Z_{macro} and Z_{micro} indicates parallelism between the two vectors and a significant correlation between patterns of morphological variation at micro- and macroevolutionary scales. We performed bootstrap tests to evaluate whether the angles between Z_{macro} and Z_{micro} were significantly < 90°, where, for each of 10 000 iterations, we resampled (with replacement) the residual size-corrected shape data (i.e. the residual relative warps) for each data-set, calculated Z_{macro} and Z_{micro} based on the resampled residuals, and then recalculated the angle between the two vectors. We note that this bootstrapping exercise allows us to account for uncertainty in the resulting divergence vectors for purposes of comparing the vectors at different taxonomic scales. The upper 5.0 percentile of these bootstrapped angles describes the one-tailed upper 95% confidence limit for the angle between Z_{macro} and Z_{micro}. If this upper confidence limit falls below 90°, the null hypothesis of no vector correlation between intra- and interspecific size-corrected vectors of divergence is rejected (Langerhans, 2009).

To visualize shape variation along the major axis of interspecific morphological divergence, we projected average cranial shapes of each species/taxonomic group onto Z_{macro}, depicting cranial shape variation for both intraspecific and interspecific datasets along a common axis using thin-plate spline transformation grids.

RESULTS

Intraspecific shape variation

Cranial shape in the *C. crocodilus*/*C. yacare* complex exhibited allometric variation, differences among taxonomic groups, and evidence for heterogeneity in multivariate allometry among taxonomic groups (Figs 2 and 3; Table 1). Visualization of allometric trends indicated that increasing centroid size was associated with a more narrow maxilla (landmarks 2–7) and increased protrusion of the nasal tip (landmark 1) in all groups within the *C. crocodilus*/*C. yacare* complex. Heterogeneity of allometry appeared to derive from a slightly steeper slope in *C. crocodilus crocodilus* compared to *C. yacare* and *C. crocodilus apaporiensis*. Nevertheless, we can examine shape variation across taxonomic groups controlling for differences in allometry for several reasons. First, the basic allometric trend within groups towards a narrowing of the snout with larger centroid size differs comparatively little across groups (i.e. the magnitude of the differences among intercepts is greater than the differences among slopes) (Fig. 2). Indeed, the multivariate effect size of heterogeneity of allometry was smaller than the main effects (Table 1). Finally, the nature of shape variation that characterized overall differences between taxonomic groups (divergence vectors derived from the taxonomic group term) was unchanged if the interaction term was removed from the model ($r = 1$), and the relative shape differences estimated between taxonomic groups were identical (same rank order), regardless of whether the interaction term was included or excluded from the model. Altogether, the minor heterogeneity in allometry had little influence on the interpretation of shape variation among taxonomic groups. For clarity, we only present results where the interaction term (centroid size × taxonomic group) was included in the analysis.

Of the four divergence vectors derived from the taxonomic group term of the MANCOVA, only the first divergence vector explained a larger proportion (93% of the predicted between-group variance) of

Table 1. Results of multivariate analyses of covariances (MANCOVA) assessing the effects of explanatory variables for cranial shape variation in the *Caiman crocodilus*/*Caiman yacare* complex

Explanatory term	*F*	d.f.	*P*	η^2 (%)
Centroid size (CS)	5.29	12, 72	< 0.0001	46.83
Taxonomic group (TG)	4.11	48, 279	< 0.0001	40.24
CS × TG	1.79	48, 279	0.0022	22.71

The MANCOVAs are based on fitting linear models where shape variables (relative warps) served as response variables and taxonomic group, centroid size, and their interaction served as explanatory variables. Statistical significance for the *F*-tests are based on Wilks's λ.

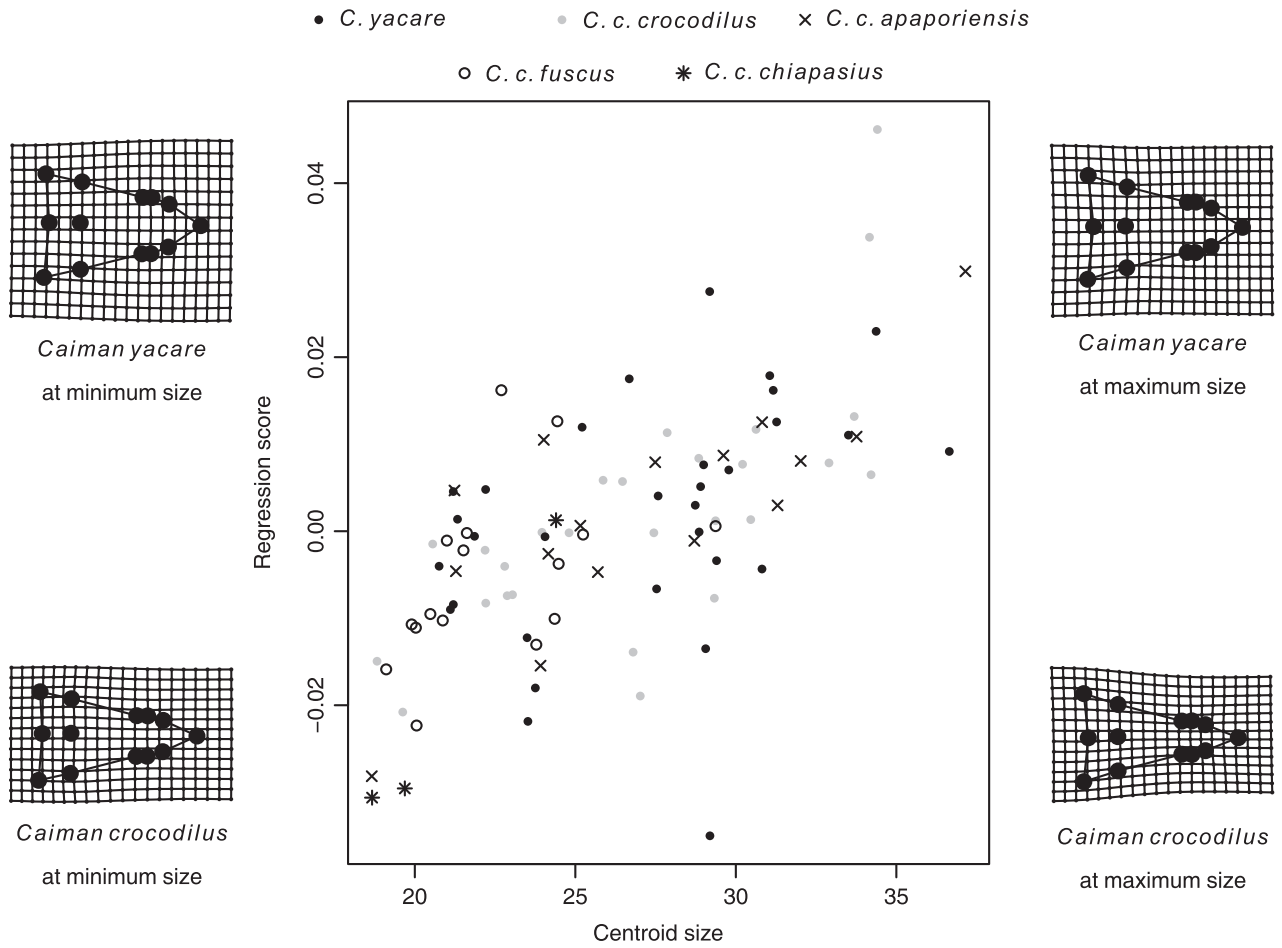

Figure 2. Multivariate allometry of cranial shape in the *Caiman crocodilus*/*Caiman yacare* complex. For all taxonomic groups, larger individuals tend to have a narrower rostrums than smaller individuals. The vertical axis describes the shape scores obtained from regressing relative warp scores against taxonomic group and centroid size (for details, see text). The predicted landmark coordinates of the largest and smallest *C. crocodilus* and *C. yacare* individuals were then mapped along with thin-plate-spline deformation grids to illustrate the shape changes relative to the average predicted shape. Although the underlying statistical analyses were performed using landmarks from one half of the crania, visualization is facilitated using thin-plate spline grids by reflecting the landmarks with bilaterally symmetric counterparts about the sagittal plane.

non-allometric shape variation than would be expected under the broken-stick model. Hence, we focus our interpretation of morphological variation among taxonomic groups on this first divergence vector. This axis describes the linear combination of relative warps that exhibit the greatest differences between groups, controlling for other terms in the model.

The first divergence vector generally described variation in the length and width of the rostrum at the anterior end of the skull, ranging from individuals with a broader, blunter snout (negative divergence vector scores) to those characterized by a narrower snout (positive scores) (Fig. 3). Thus, both the first divergence vector and the allometric component of variation characterize a common gradient from narrow- to broad-snouted forms, indicating a major morphological gradient in the data. Variation in the landmarks determining the width of the maxilla (landmarks 2–7) and the protrusion of the nasal tip (landmark 1) largely drive the first divergence vector (Fig. 3). Controlling for allometry, *C. crocodilus apaporiensis* exhibited a much narrower snout, whereas *C. crocodilus fuscus* and *C. yacare* tended to have broader snouts for a given cranial size. *Caiman crocodilus chiapasius* exhibited somewhat intermediate skull shapes, and *C. crocodilus crocodilus* exhibited considerable variation spanning a large range of the shape space described by the divergence vector. Rather than representing an extreme form

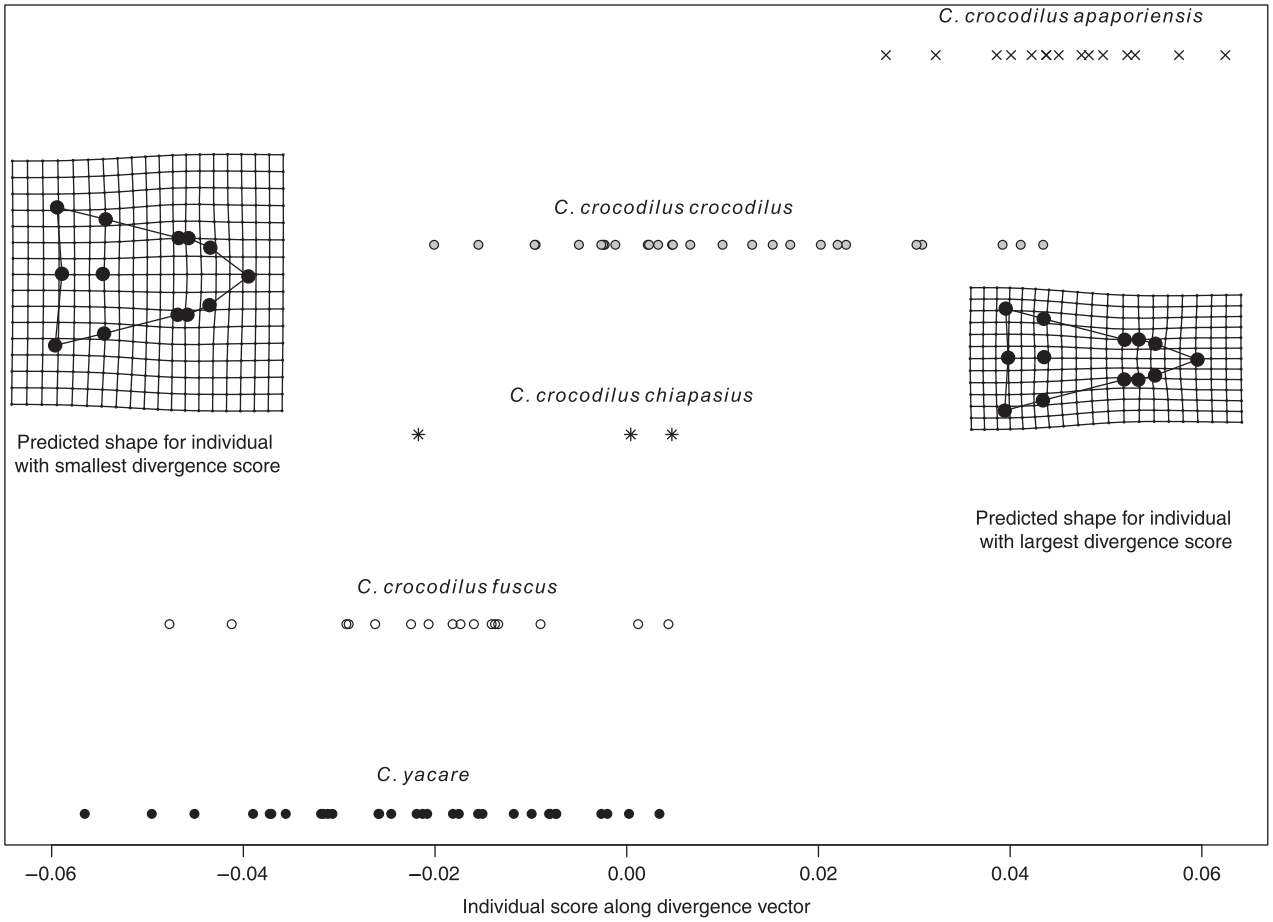

Figure 3. Cranial shape differences across taxonomic groups, controlling for the effects of allometry. The values on the horizontal axis are the scores for the first divergence vector associated with the taxonomic group term from the multivariate analysis of covariance describing shape variation across taxonomic groups. Thus, the values represent the primary manner in which taxonomic groups differ in cranial shape, controlling for allometric variation. Cranial shape differences are shown with thin-plate spline transformation grids of the predicted shape relative to the mean set of landmarks.

within the complex, *C. yacare* spanned a considerable range of shape variation along the divergence vector, with its mean nested within the subspecies of *C. crocodilus*. This finding supports our inclusion of *C. yacare* within a *C. crocodilus*/*C. yacare* complex, although all results are very similar if we exclude *C. yacare* (see Supporting information, Data S1).

Comparison with interspecific shape variation

For the interspecific data, Z_{macro} (the first PC of the size-corrected residual relative warp scores for the interspecific data set) distinguished broad-snouted taxa (e.g. *C. latirostris* and *Melanosuchus niger*) from narrow-snouted taxa (e.g. *Mecistops cataphractus* and *C. johnsoni*) (Fig 4A), capturing cranial shape variation ranging from short, broad and blunt skulls (negative scores) to narrow and acute skulls (positive scores) relative to overall skull size. Thus, Z_{macro} had a strong qualitative resemblance to patterns uncovered in the intraspecific analysis, with species with narrower and acute skulls being characterized by a more protruded nasal tip and a narrower maxilla.

Our quantitative comparison between Z_{macro} and Z_{micro} showed the angle between the two axes to be very low (41.2°), differing significantly from 90° (Fig. 4B) (upper 95% confidence limit of 57.4°). Thus, the direction of cranial shape variation among crocodilians at the interspecific level is highly similar to the gradient of variation among taxonomic groups within the *C. crocodilus*/*C. yacare* complex. Projecting the average shapes for taxonomic groups within the *C. crocodilus*/*C. yacare* complex onto the

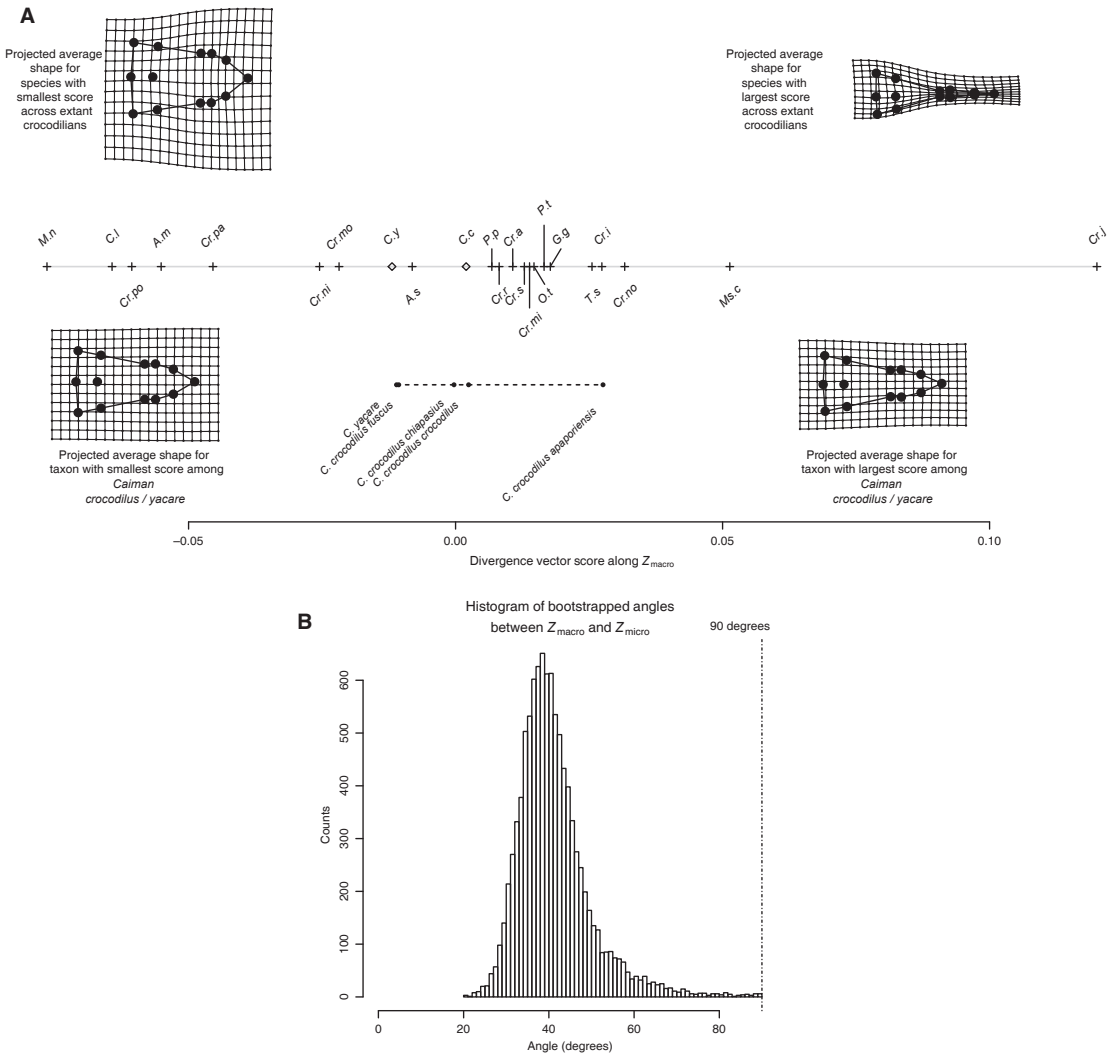

Figure 4. A, occupation along Z_{macro}, the first principal component of the non-allometric component of the relative warps for the interspecific dataset derived from Pearcy & Wijtten (2011) (cross marks on solid, grey line). The data points for the mean *Caiman crocodilus* and *Caiman yacare* skulls from Pearcy & Wijtten (2011) (open square, grey line) were projected a posteriori onto Z_{macro} derived from the interspecific dataset with these datapoints excluded. Average skull shape for each taxonomic group within the *C. crocodilus*/*C. yacare* complex (black dots on dashed line) was projected onto this axis to permit the comparison of the non-allometric component of shape variation in both groups along a common axis. Taxa: A.m, *Alligator mississippiensis*; A.s, *Alligator sinensis*; C.l, *Caiman latirostris*; C.c, *Caiman crocodilus*; C.l, *Caiman yacare*; Cr.a, *Crocodylus acutus*; Ms.c, *Mecistops cataphractus*; Cr.i, *Crocodylus intermedius*; Cr.j, *Crocodylus johnsoni*; Cr.mi, *Crocodylus mindorensis*; Cr.mo, *Crocodylus moreletii*; Cr.ni, *Crocodylus niloticus*; Cr.no, *Crocodylus noveaguinea*; Cr.po, *Crocodylus porosus*; Cr.rh, *Crocodylus rhombifer*; Cr.s, *Crocodylus siamensis*; G.g, *Gavialis gangeticus*; M. n, *Melanosuchus niger*; O. t, *Osteolamus tetrapsis*; P. p, *Paleosuchus palpebrosus*; P. t, *Paleosuchus trigonatus*; T.s, *Tomistoma schlegii*. We emphasize that the arrangement of species along the interspecific divergence vector results from our characterization of shape differences because of removal of the effect of allometric variation. B, bootstrapped distribution (from 10 000 iterations) of the angles between Z_{macro} and Z_{micro}.

interspecific divergence vector revealed that the intraspecific groups exhibit a large range of shape variation, spanning the average skull shapes for 11 out of 21 other species of extant crocodilians (Fig. 4A).

DISCUSSION

The results of the present study provide strong quantitative support for the hypothesis that cranial shape variation within the *C. crocodilus*/*C. yacare* complex (or within *C. crocodilus*, excluding *C. yacare*; see Sup-

porting information, Data S1), controlling for allometry, lies along a continuum ranging from broad- to narrow-snouted phenotypes reminiscent of the pattern found across both extant and extinct crocodilian species (Medem, 1955, 1981, 1983; Ayarzagüena, 1984; Gorzula, 1994). We found substantial cranial shape diversity within the *C. crocodilus*/*C. yacare* complex, even when compared with standing patterns of morphological variation across extant crocodilians. The strong vector correlation between the major axes of cranial shape diversification across micro- and macroevolutionary scales is consistent with the idea that the mechanisms underlying intraspecific phenotypic divergence (differentiation within the *C. crocodilus*/*C. yacare* complex) can potentially scale up to explain patterns of diversification at higher taxonomic levels (across all extant crocodilians). This result also shows how the primary gradient of morphological differentiation between species can become apparent over microevolutionary time scales.

Analyzing diversity in crocodilian cranial shapes with geometric morphometrics allowed a quantitative comparison of patterns of diversification across different taxonomic hierarchies (Busbey, 1997; Pierce *et al.*, 2008; Piras *et al.*, 2009; Pearcy & Wijtten, 2011). Using a common set of landmarks employed by a previous study assessing cranial shape variation (Pearcy & Wijtten, 2011), we could directly place patterns of intraspecific variation within the context of earlier work focusing on interspecific variation. Our geometric morphometric approach could also potentially be useful in suggesting morphological criteria for demarcating different taxonomic groups within *C. crocodilus*. The first two relative warps alone correctly classify a mean of approximately 82% of leave-one-out cross-validated *C. crocodilus apaporiensis* specimens (see Supporting information, Data S4).

Following the focus of previous studies on adult and sub-adult morphology (Pierce *et al.*, 2008; Pearcy & Wijtten, 2011), we excluded very young individuals from our analysis, precluding evaluating patterns of ontogenetic variation in *C. crocodilus*. However, our finding that larger individuals exhibit a narrowing of the skull in *C. crocodilus crocodilus* is consistent with previous work including very small individuals (Monteiro, Cavalcanti & Sommer, 1997). In a study of ontogenetic shape-changes among *Caiman* species (*C. latirostris*, *C. yacare*, and *C. crocodilus*), Monteiro *et al.* (1997) showed that the pattern of ontogenetic shape change differs between *C. latirostris* and the other *Caiman* species: *C. yacare* and *C. crocodilus* exhibited some cranial elongation and narrowing later in development, whereas *C. latirostris* exhibited a slight broadening of the rostrum during development. In light of the results reported in the present study and those of Monteiro *et al.* (1997), the comparison of ontogenetic cranial shape changes between *C. crocodilus* populations and subspecies, particularly those from different ends of the continuum of snout shape differences, represents a promising avenue for further research.

We also note that, because museum specimens are often collected in the field, observed patterns of variation can still partially reflect developmental differences that arise from individuals living in different environments (phenotypic plasticity). Uncovering the relative importance of phenotypic plasticity and genetic divergence, and their joint roles in crocodilian diversification (Pfennig & Pfennig, 2010), deserves future study. For example, subspecies exhibiting higher levels of phenotypic plasticity can potentially establish broader geographical ranges (Ernande & Dieckmann, 2004) and render some subspecies more prone to local adaptation (Kawecki & Ebert, 2004), accentuating morphological diversification in these groups. Comparing patterns of intraspecific variation between widely-distributed crocodilian species (e.g. *C. crocodilus* and *Crocodylus niloticus*) and species more narrowly endemic to smaller geographical regions (e.g. *Crocodylus rhombifer*, *Alligator sinensis*) may help interpret the role that an expanded geographical range plays in generating cranial shape differences in crocodilians.

Our findings that substantial intraspecific variation in *Caiman crocodilus* skulls (relative to interspecific variation) exists and parallels interspecific patterns of crocodilian skull shape variation may potentially inform efforts to clarify the evolutionary dynamics of cranial morphological diversification in crocodilians as a whole. For example, competition for food may promote diversification in feeding morphology, whether within populations as resource polymorphisms, across allopatric populations or for different (potentially incipient) species co-occurring in sympatry experiencing ecological character displacement (Brown & Wilson, 1956; Robinson & Wilson, 1994; Smith & Skulason, 1996; Adams & Rohlf, 2000; Schluter, 2000b; Wainwright, 2007; Pfennig & Pfennig, 2010). Previous work supports the hypothesis that variation in cranial shape influences the ability of individuals to capture and consume different types of prey, with studies suggesting that adaptive diversification in feeding and foraging strategies largely explains macroevolutionary patterns of skull shape variation in crocodilians (Busbey, 1997; Cleuren & de Vree, 2000; McHenry *et al.*, 2006; Pierce *et al.*, 2008).

The fact that cranial shape varies so widely within *C. crocodilus* along a continuum ranging from narrow- to broad-snouted morphs, even compared to standing patterns of interspecific variation, suggests that crocodilian cranial shape, and the rostrum in particular, may represent a highly evolvable trait

exhibiting high levels of expected evolutionary responses to selection on features such as cranium width (Houle, 1992; Hansen, Pélabon & Houle, 2011), although the extent of differentiation that a given lineage may undergo may be subject to developmental or allometric constraints (Zelditch *et al.*, 2003; Smith *et al.*, 2004). Replicated evolution of similar skull shapes in multiple lineages and little phylogenetic signal for skull morphology constitute well-established macroevolutionary patterns in crocodilians. Moreover, the high levels of intraspecific phenotypic variation uncovered in the present study align with the principal direction of macroevolutionary diversification in crocodilian cranial shape. Taken together, these facts suggest two key points. First, cranial shape is likely to exhibit especially high evolvability (with considerable variation, relative to interspecific variability, potentially evolving rapidly within a single species). Second, there could be especially strong selection along the narrow-broad snouted continuum. These possibilities are not mutually exclusive, and a promising angle for future investigation would be determining whether the primary axes of variability uncovered in the present study align with 'genetic lines of least resistance' (Schluter, 1996). Such an alignment could help explain the consistency of diversification across micro- and macroevolutionary scales. Regardless of its underlying causes, the results of the present study illustrate how patterns of phenotypic differentiation observable during early stages of divergence within a species can scale up to inform broader macroevolutionary patterns.

ACKNOWLEDGEMENTS

This research was funded in part by a Chair's Fellowship from the Department of Ecology and Evolutionary Biology at the University of California, Los Angeles. We would like to thank N. Camacho, J. Jacobs, K. Kelly, D. Kizirian, K. Krysko, M. Nickerson, R. Pascocello, A. Resetar, K. Tighe, and A. Wynn for their gracious hospitality and help with accessing the collections; A. Stein for assistance with photography; C. Brochu for sharing specimen images; M. Fritz and C. Arellano for helpful discussion; and G. Grether, C. Brochu, and the anonymous reviewers for providing valuable comments on earlier versions of the manuscript.

REFERENCES

Adams DC, Otárola-Castillo E. 2013. Geomorph: an R package for the collection and analysis of geometric morphometric shape data. *Methods in Ecology and Evolution* **4:** 393–399.

Adams DC, Rohlf FJ. 2000. Ecological character displacement in plethodon: biomechanical differences found from a geometric morphometric study. *Proceedings of the National Academy of Sciences of the United States of America* **97:** 4106–4111.

Arnold SJ, Pfrender ME, Jones AG. 2001. The adaptive landscape as a conceptual bridge between micro- and macroevolution. *Genetica* **112–113:** 9–32.

Ayarzagüena J. 1984. Variaciones En La Dieta de *Caiman Sclerops*. La Relacion Entre Morfologia Bucal Y Dieta. *Memoria De La Sociedad De Ciencias Naturales La Salle* **44:** 123–140.

Bookstein FL 1997. *Morphometric tools for landmark data: geometry and biology*. Cambridge: Cambridge University Press.

Brochu CA. 1997. Morphology, fossils, divergence timing, and the phylogenetic relationships of *Gavialis*. *Systematic Biology* **46:** 479–522.

Brochu CA. 2003. Phylogenetic approaches toward Crocodylian history. *Annual Review of Earth Planetary Sciences* **31:** 357–397.

Brochu CA 2001. Crocodylian snouts in space and time: phylogenetic approaches toward adaptive radiation. *American Zoologist* **41:** 564–585.

Brown WL, Wilson EO. 1956. Character displacement. *Systematic Biology* **5:** 49–65.

Busack SD, Pandya S. 2001. Geographic variation in *Caiman crocodilus* and *Caiman yacare* (Crocodylia: Alligatoridae): systematic and legal implications. *Herpetologica* **57:** 294–312.

Busbey AB. 1997. The structural consequences of skull flattening in Crocodilians. In: Thomason JJ, ed. *Functional morphology in vertebrate paleontology*. New York, NY: Cambridge University Press, 173–192.

Calsbeek R, Smith TB, Bardeleben C. 2007. Intraspecific variation in *Anolis Sagrei* mirrors the Adaptive Radiation of Greater Antillean Anoles. *Biological Journal of the Linnean Society* **90:** 189–199.

Cleuren J, de Vree F. 2000. Feeding in crocodilians. In: Schwenk K, ed. *Feeding: form, function, and evolution in tetrapod vertebrates*. New York, NY: Academic Press, 337–358.

Darwin C. 1859. *On the origin of species*. London: John Murray.

Dobzhansky T. 1937. *Genetics and the origin of species*. New York, NY: Columbia University Press.

Drake AG, Klingenberg P. 2008. The pace of morphological change: historical transformation of skull shape in St bernard dogs. *Proceedings of the Royal Society of London Series B, Biological Sciences* **275:** 71–76.

Dryden I. 2012. Shapes: Statistical Shape Analysis. Available at: http://cran.r-project.org/package=shapes.

Elmer KR, Meyer A. 2011. Adaptation in the age of ecological genomics: insights from parallelism and convergence. . *Trends in Ecology and Evolution* **26:** 298–306.

Ernande B, Dieckmann U. 2004. The evolution of phenotypic plasticity in spatially structured environments: implications of intraspecific competition, plasticity costs and

environmental characteristics. *Journal of Evolutionary Biology* **17:** 613–628.

Firmat C, Schliewen UK, Losseau M, Alibert P. 2012. Body shape differentiation at global and local geographic scales in the invasive cichlid *Oreochromis mossambicus*. *Biological Journal of the Linnean Society2* **105:** 369–381.

Franssen NR. 2011. Anthropogenic habitat alteration induces rapid morphological divergence in a native stream fish. *Evolutionary Applications* **4:** 791–804.

Franssen NR, Stewart LK, Schaefer JF. 2013. Morphological divergence and flow-induced phenotypic plasticity in a native fish from Anthropogenically altered stream habitats. *Ecology and Evolution* **3:** 4648–4657.

Frontier S. 1976. Étude de La Décroissance Des Valeurs Propres Dans Une Analyse En Composantes Principales: comparaison Avec Le Moddle Du Bâton Brisé. *Journal of Experimental Marine Biology and Ecology* **25:** 67–75.

Gingerich PD. 2001. Rates of evolution on the time SCALE of the evolutionary process. *Genetica* **112–113:** 127–144.

Glor RE. 2010. Phylogenetic insights on adaptive radiation. *Annual Review of Ecology, Evolution, and Systematics* **41:** 251–270.

Gorzula S. 1994. A Longirostrine *Caiman crocodilus* from central Venezuela. *Crocodile Specialist Group* **13:** 16.

Gould SJ. 2002. *The structure of evolutionary theory*. Cambridge, MA: Beknap Press of Harvard University Press.

Hall PM, Portier KM. 1994. Cranial morphometry of new guinea crocodiles (*Crocodylus Novaeguineae*): ontogenetic variation in relative growth of the skull and an assessment of Its utility as a predictor of the sex and size of individuals. *Herpetological Monographs* **8:** 203–225.

Hansen TF, Pélabon C, Houle D. 2011. Heritability is not evolvability. *Evolutionary Biology* **38:** 258–277.

Houle D. 1992. Comparing evolvability and variability of quantitative traits. *Genetics* **130:** 195–204.

Hrbek T, Rangel Vasconcelos W, Rebelo G, Pires Farias I. 2008. Phylogenetic relationships of South American alligatorids and the caiman of Madeira River. *Journal of Experimental Zoology Part A: Ecological Genetics and Physiology* **309A:** 588–599.

Jackson DA. 1993. Stopping rules in principal components analysis: a comparison of heuristical and statistical approaches. *Ecology* **74:** 2204–2214.

Kawecki TJ, Ebert D. 2004. Conceptual issues in local adaptation. *Ecology Letters* **7:** 1225–1241.

King FW, Burke RL. 1989. *Crocodilian, tuatara, and turtle species of the world: a taxonomic and geographic reference*. Washington, DC: Association of Systematics Collections.

Kinnison MT, Hendry AP. 2001. The pace of modern life II: from rates of contemporary microevolution to pattern and process. *Genetica* **112–113:** 145–164.

Klingenberg CP 1996. Multivariate allometry. In: Marcus LF, Corti M, Loy A, Naylor GJP, Slice DE, eds. *Advances in morphometrics, Vol. 284*. New York, NY: Plenum Press, 23–49.

Langerhans RB. 2009. Trade-off between steady and unsteady swimming underlies predator-driven divergence in Gambusia affinis. *Journal of Evolutionary Biology* **22:** 1057–1075.

Langerhans RB, DeWitt TJ. 2004. Shared and unique features of evolutionary diversification. *American Naturalist* **164:** 335–349.

Langerhans RB, Makowicz AM. 2009. Shared and unique features of morphological differentiation between predator regimes in Gambusia caymanensis. *Journal of Evolutionary Biology* **22:** 2231–2242.

Legendre P, Legendre L. 1998. *Numerical ecology, Vol. 20*. Amsterdam: Elsevier Science.

MacArthur RH. 1957. On the relative abundance of bird species. *Proceedings of the National Academy of Sciences of the United States of America* **43:** 293–295.

McHenry CR, Clausen PD, Daniel WJT, Meers MB, Pendharkar A. 2006. Biomechanics of the rostrum in crocodilians: a comparative analysis using finite-element modeling. *The Anatomical Record Part A: Discoveries in Molecular, Cellular, and Evolutionary Biology* **288A:** 827–849.

Medem F. 1955. A new subspecies of *Caiman Sclerops* from Colombia. *Fieldiana. Zoology* **37:** 339–343.

Medem F. 1981. *Los Crocodylia de Sur America Volumen I*. Bogotá: Ministerio de Educación Nacional.

Medem F. 1983. *Los Crocodylia de Sur America Volumen II*. Bogotá: Ministerio de Educación Nacional.

Moczek AP. 2006. Integrating micro- and macroevolution of development through the study of horned beetles. *Heredity* **97:** 168–178.

Monnet C, De Baets K, Klug C. 2011. Parallel evolution controlled by adaptation and covariation in ammonoid cephalopods. *BMC Evolutionary Biology* **11:** 115.

Monteiro LR, Soares M. 1997. Allometric analysis of the ontogenetic variation and evolution of the skull in *Caiman Spix*, 1825 (Crocodylia: Alligatoridae). *Herpetologica* **53:** 62–69.

Monteiro LR, Cavalcanti MJ, Sommer HJS. 1997. Comparative ontogenetic shape changes in the skull of *Caiman* species (Crocodylia, Alligatoridae). *Journal of Morphology* **231:** 53–62.

Oaks JR. 2011. A time-calibrated species tree of Crocodylia reveals a recent radiation of the true crocodiles. *Evolution* **65:** 3285–3297.

Pearcy A, Wijtten Z. 2011. A morphometric analysis of crocodilian skull shapes. *The Herpetological Journal* **21:** 213–218.

Pfennig DW, Pfennig KS. 2010. Character displacement and the origins of diversity. *American Naturalist* **176:** S26–S44.

Pierce SE, Angielczyk KD, Rayfield EJ. 2008. Patterns of morphospace occupation and mechanical performance in extant Crocodilian skulls: a combined geometric morphometric and finite element modeling approach. *Journal of Morphology* **269:** 840–864.

Piras P, Teresi L, Buscalioni AD, Cubo J. 2009. The shadow of forgotten ancestors differently constrains the fate of

Alligatoroidea and Crocodyloidea. *Global Ecology and Biogeography* **18:** 30–40.

Platt SG, Rainwater TR, Thorbjarnarson JB, Finger AG, Anderson TA, McMurry ST. 2009. Size estimation, morphometrics, sex ratio, sexual size dimorphism, and biomass of Morelet's crocodile in Northern Belize. *Caribbean Journal of Science* **45:** 80–93.

Robinson BW, Wilson DS. 1994. Character release and displacement in fishes: a neglected literature. *American Naturalist* **144:** 596.

Rohlf FJ. 2005. *TpsDig 2*. Stoney Brook, NY: Department of Ecology; Evolution, State Univeristy of New York.

Rohlf FJ, Marcus LF. 1993. A revolution in morphometrics. *Trends in Ecology and Evolution* **8:** 129–132.

Ross JP. 1998. *Crocodiles: status survey and conservation action plan, 2nd edn.*International Union for Conservation of Nature. Gland, Switzerland: Natural Resources.

Rüber L, Verheyen E, Meyer A. 1999. Replicated evolution of trophic specializations in an endemic cichlid fish lineage from lake tanganyika. *Proceedings of the National Academy of Sciences of the United States of America* **96:** 10230–10235.

Sadleir RW, Makovicky PJ. 2008. Cranial shape and correlated characters in Crocodilian evolution. *Journal of Evolutionary Biology* **21:** 1578–1596.

Saxer G, Doebeli M, Travisano M. 2010. The repeatability of adaptive radiation during long-term experimental evolution of *Escherichia Coli* in a multiple nutrient environment. *PLoS ONE* **5:** e14184.

Scheyer TM, Aguilera OA, Delfino M, Fortier DC, Carlini AA, Sánchez R, Carrillo-Briceño JD, Quiroz L, Sánchez-Villagra MR. 2013. Crocodylian diversity peak and extinction in the late Cenozoic of the northern Neotropics. *Nature Communications* **4:** 1907.

Schluter D. 1996. Adaptive radiation along genetic lines of least resistance. *Evolution* **50:** 1766–1774.

Schluter D. 2000a. Ecological character displacement in adaptive radiation. *American Naturalist* **156:** S4–S16.

Schluter D. 2000b. *The Ecology of Adaptive Radiation*. Oxford: Oxford University Press.

Simpson G. 1944. *Tempo and Mode in Evolution*. New York, NY: Columbia University Press.

Smith TB, Skulason S. 1996. Evolutionary significance of resource polymorphisms in fishes, amphibians, and birds. *Annual Review of Ecology and Systematics* **27:** 111–133.

Smith FA, Brown JH, Haskell JP, Lyons SK, Alroy J, Charnov EL, Dayan T, Enquist BJ, Ernest SK, Hadly EA, Jones KE, Kaufman DM, Marquet PA, Maurer BA, Niklas KJ, Porter WP, Tiffney B, Willig MR. 2004. Similarity of mammalian body size across the taxonomic hierarchy and across space and time. *American Naturalist* **163:** 672–691.

Stanley SM. 1979. *Macroevolution*. Baltimore, MD: The Johns Hopkins University Press.

Uyeda JC, Hansen TF, Arnold SJ, Pienaar J. 2011. The million-year wait for macroevolutionary bursts. *Proceedings of the National Academy of Sciences of the United States of America* **108:** 15908–15913.

Venegas-Anaya M, Crawford AJ, Escobedo Galván AH, Sanjur OI, Densmore LD, Bermingham E. 2008. Mitochondrial DNA phylogeography of *Caiman crocodilus* in mesoamerica and South America. *Journal of Experimental Zoology Part A: Ecological Genetics and Physiology* **309A:** 614–627.

Verdade LM. 1999. Regression equations between body and head measurements in the broad-snouted caiman. *Revista Brasileira de Biologia* **60:** 469–482.

Wainwright PC. 2007. Functional versus morphological diversity in macroevolution. *Annual Review of Ecology, Evolution and Systematics* **38:** 381–401.

Webb GJW, Messel H. 1978. Morphometric analysis of *Crocodylus Porosus* from the north coast of Arnhem Land, northern Australia. *Australian Journal of Zoology* **26:** 1–27.

Wu XB, Xue H, Wu LS, Zhu JL, Wang RP. 2006. Regression analysis between body and head measurements of chinese alligators (*Alligator Sinensis*) in the captive population. *Animal Biodiversity and Conservation* **29:** 65–71.

Zelditch ML, Sheets HD, Fink WL. 2003. The ontogenetic dynamics of shape disparity. *Paleobiology* **29:** 139–156.

SUPPORTING INFORMATION

Additional Supporting Information may be found in the online version of this article at the publisher's web-site:

Figure S1. Geographical variation along the divergence vector derived from the taxonomic group term for the multivariate analysis of covariance.

Figure S2. The distribution of cranial shapes for extant crocodilians along the first two interspecific principal component axes derived from the MANCOVA using only interspecific data.

Data S1. Analyses exclusive of *Caiman yacare* specimens.

Data S2. Catalog ID, or relevant figure from Medem (1983), and details of specimens used in the analysis.

Data S3. Statistical analyses of the effects of approximate life stage and sex.

Data S4. Discriminating *Caiman crocodilus apaporiensis* and *Caiman yacare* specimens.

Supplementary Figure S1 - Geographic variation along the divergence vector derived from the taxonomic group term for the MANCOVA

The occupation of morphological space controlling for allometric effects in *Caiman crocodilus* along the major divergence vector according to the geographic areas from which the samples were collected for (A) *Caiman crocodilus crocodilus* (B) *Caiman crocodilus chiapasius*, (C) *Caiman crocodilus fuscus* and (D) *Caiman crocodilus apaporiensis*. For *Caiman crocodilus*, the geographic area where the specimens were collected were available for the specimens included in the analysis to the first level administrative districts (e.g., provinces and states) of the countries in which the specimens were collected. These areas and their abbreviations are: Acre, Brazil (AB), Amazonas, Colombia (AC), Barinas, Venezuela (BaV), Bolívar, Venezuela (BV), Bocas del Toro, Panama (BP), Boyacá, Colombia (BC). Caquetá, Colombia (QC), Casanare, Colombia (CaC), Cauca, Colombia (CuC), Chiapas, Mexico (CMX), Chocó, Colombia (ChC), Cojedes, Venezuela (CV), Córdoba, Colombia (CoC), Guárico, Venezuela (GV), Magdalena, Colombia (MaC), Meta, Colombia (MC), Monagas, Venezuela (MV), Panama Canal Zone, Panama (PCP), Putumayo, Colombia (PuC), Vaupés, Colombia (VaC), Vichada, Colombia (VC) and Zulia, Venezuela (ZV).

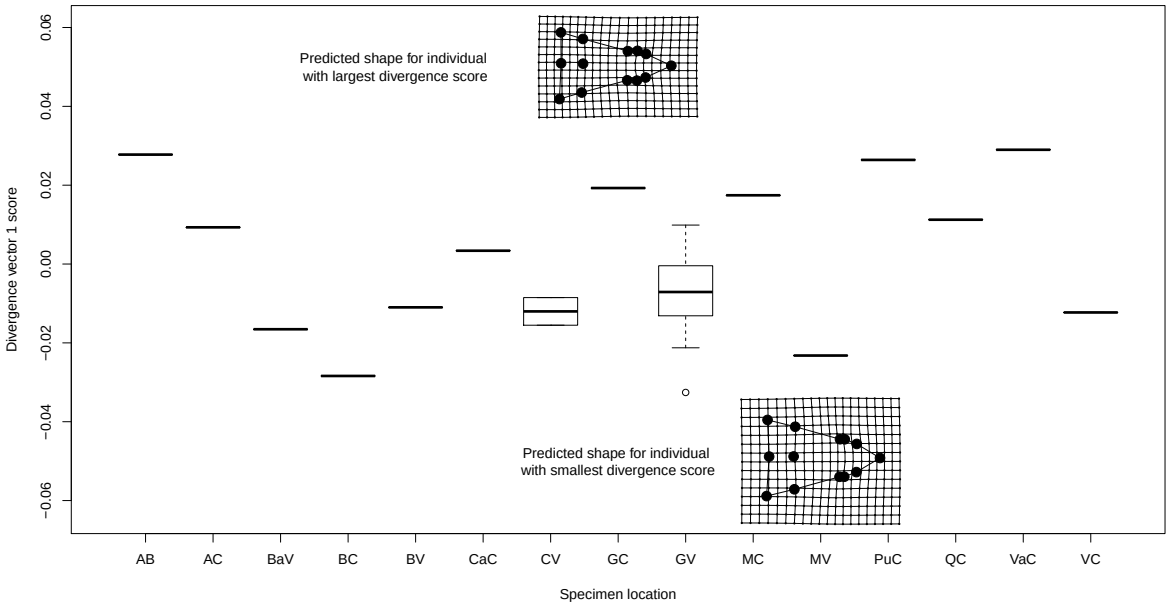
Predicted shape for individual
with largest divergence score
Predicted shape for individual
with smallest divergence score
Divergence vector 1 score
0.06
0.04
0.02
0.00
−0.02
−0.04
−0.06
AB
AC
BaV
BC
BV
CaC
CV
GC
GV
MC
MV
PuC
QC
VaC
VC
Specimen location

A

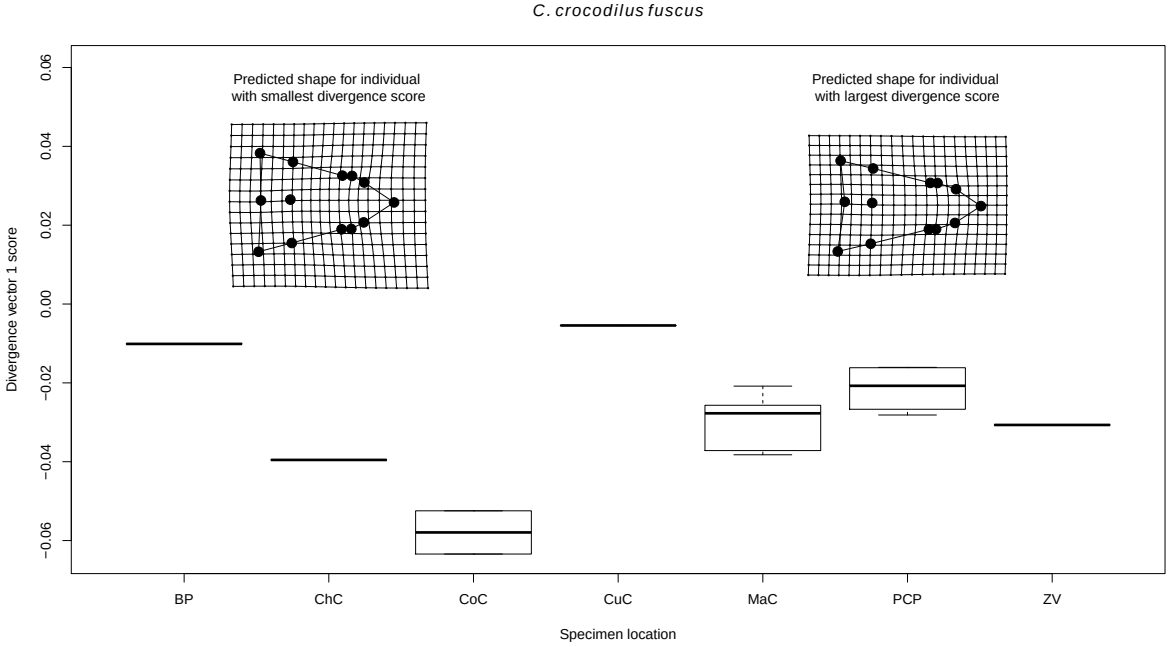
C. crocodilus fuscus
Predicted shape for individual with smallest divergence score
Predicted shape for individual with largest divergence score
Divergence vector 1 score
0.06
0.04
0.02
0.00
−0.02
−0.04
−0.06
BP
ChC
CoC
CuC
MaC
PCP
ZV
Specimen location

B

C. crocodilus chiapasius

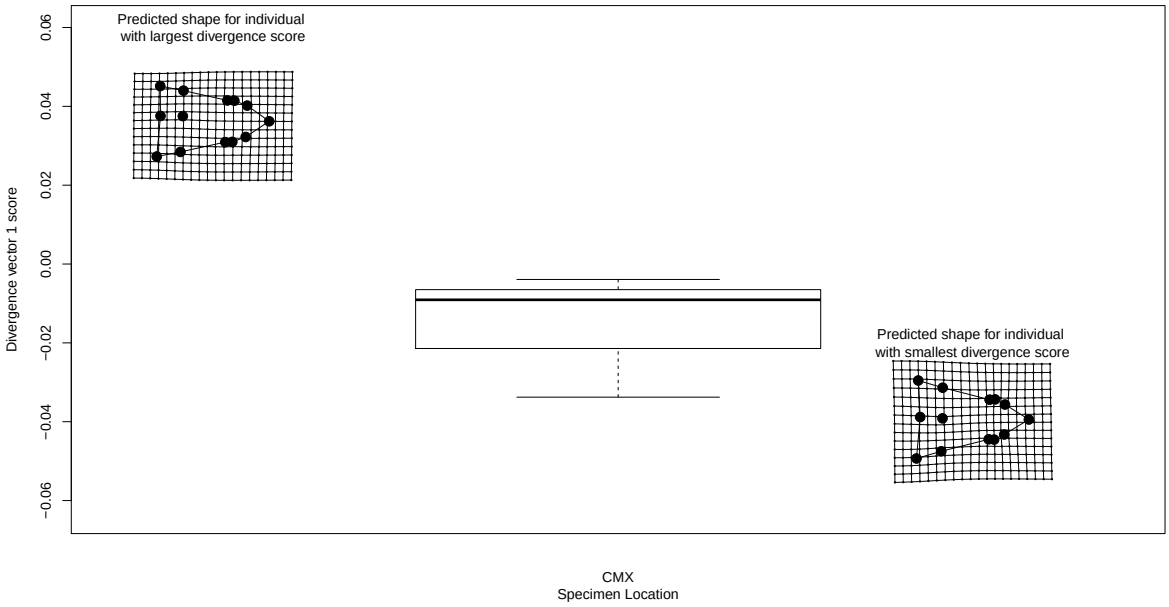

C

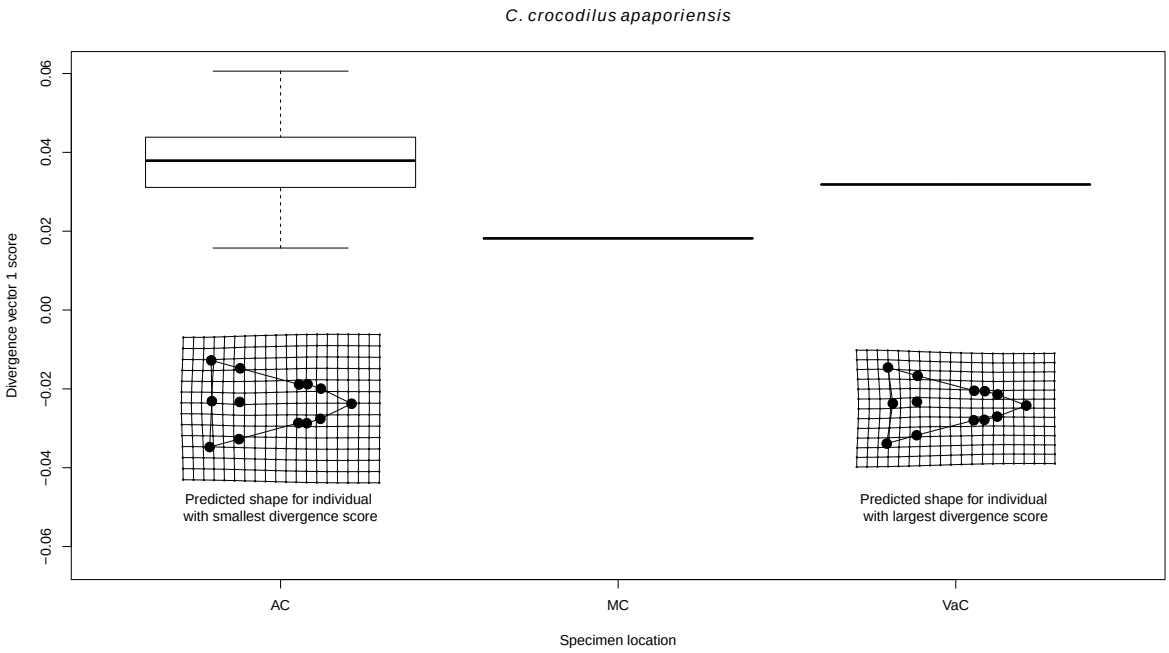
C. crocodilus apaporiensis
Divergence vector 1 score
0.06
0.04
0.02
0.00
−0.02
−0.04
−0.06
Predicted shape for individual
with smallest divergence score
Predicted shape for individual
with largest divergence score
AC
MC
VaC
Specimen location

D

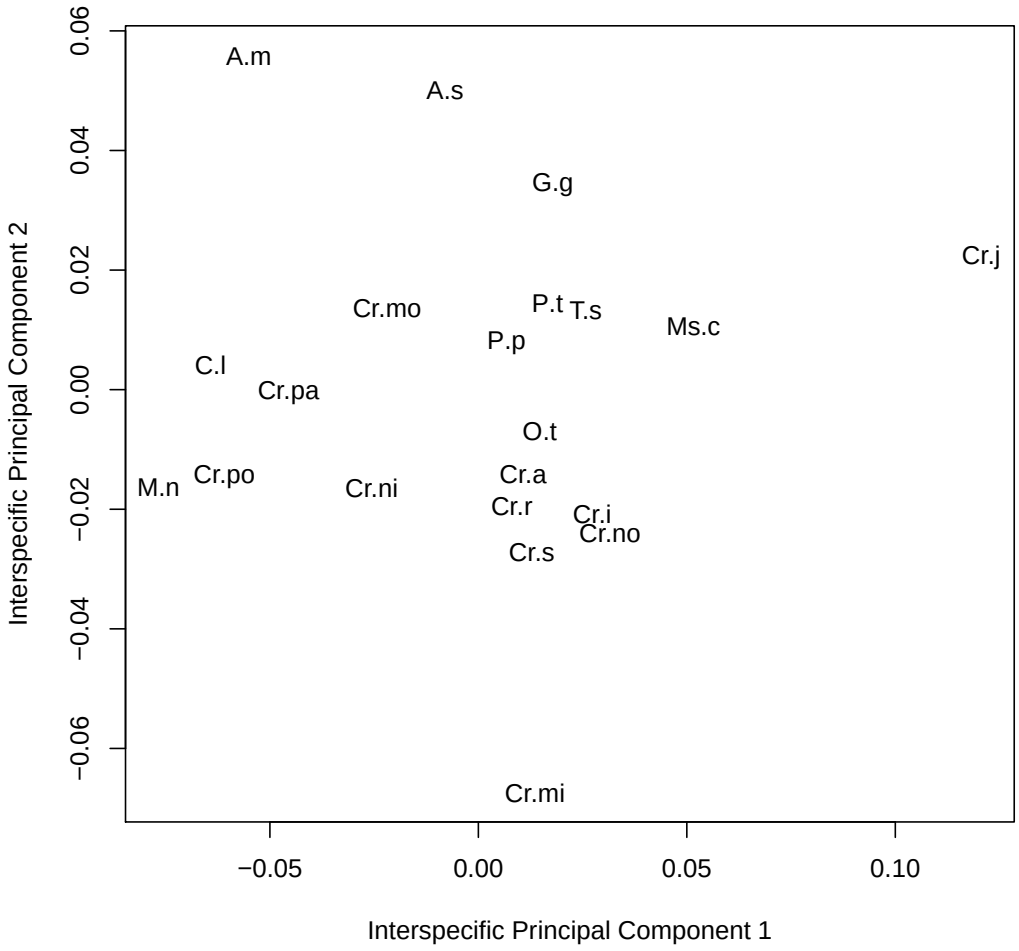

Supplementary Figure S2. The distribution of cranial shapes for extant crocodilians along the first two interspecific principal component axes derived from the MANCOVA using only interspecific data. Only these PCs were found to explain a higher share of variance than expected under the broken stick model. The taxa are abbreviated as A.m (*Alligator mississippiensis*), A.s (*Alligator sinensis*), C.l (*Caiman latirostris*), Cr.a (*Crocodylus acutus*), Ms.c (*Mecistops cataphractus*), Cr.i (*Crocodylus intermedius*), Cr.j (*Crocodylus johnsoni*), Cr.mi (*Crocodylus mindorensis*), Cr.mo (*Crocodylus moreletii*), Cr.ni (*Crocodylus niloticus*), Cr.no (*Crocodylus noveaguinea*), Cr.po (*Crocodylus porosus*), Cr.rh (*Crocodylus rhombifer*), Cr.s (*Crocodylus siamensis*), G.g (*Gavialis gangeticus*), M. n (*Melanosuchus niger*), O. t (*Osteolamus tetrapsis*), P. p (*Paleosuchus palpebrosus*), P. t (*Paleosuchus trigonatus*), and T.s (*Tomistoma schlegii*).

1

Supplementary Information S1 - Analyses exclusive of *Caiman yacare* specimens

Analysis of intra-specific shape variation without *Caiman yacare* specimens

We conducted MANCOVA as described in the main text, with the exception that we excluded all specimens of *C. yacare* from the analysis. We found significant allometric effects, differences among *C. crocodilus* subspecies, and heterogeneous multivariate allometry among subspecies (Table S1). The effect of centroid size variation on the regression scores **s** generated by projecting the relative warps onto a regression vector for centroid size was virtually identical to the analysis presented in the main text, which included *C. yacare* (Supplementary Figure S1-a; see the main text for methodological details). As in the analysis in the main text, specimens with larger centroid sizes tended to have narrower maxilla (landmarks 2-7) and increased protrusion of the nasal tip (landmark 1) across groups, with *C. c. crocodilus* exhibiting the largest heterogeneities in allometry. As in the case with *C. yacare* included in the analysis, these results demonstrate that shape variation independent of allometry could be meaningfully interpreted for the same reasons as described in the main text.

Only the first divergence vector associated with the taxonomic group term in the MANCOVA explained a larger proportion of variation than expected under the broken-stick model (= 93.9%; Legendre and Legendre 1998). Thus, as in our analysis in the main text, we again focus on the first divergence vector of the taxonomic group term to illustrate morphological differences among groups. Figure S1-b illustrates shape variation within *Caiman crocodilus*, controlling for allometry, along the first divergence vector. Again, the distribution of individual *C. crocodilus* cranial shapes spanned a continuum ranging from longirostrine to broad-snouted morphs, with *C. crocodilus apaporiensis* strongly clustered on the longirostrine end of the continuum and *C. crocodilus fuscus* clustered on the broad-snouted end (Figure S1-b).

Comparison to Interspecific shape variation

As described in the main text, we base our comparison of the major axes of cranial shape variation between the intra-specific and inter-specific data on the residual relative warp scores

from a multivariate regression of relative warps on centroid size separately for each taxonomic scale (interspecific and intraspecific). The first principal component of the residual average relative warp scores, controlling for intraspecific allometry within *Caiman crocodilus*, exclusive of *Caiman yacare*, accounted for $\approx 87\%$ of intra-specific average shape variation, and was the only PC to explain a higher proportion of cranial morphological diversity than expected under a broken-stick model. As was the case with the analysis including *C. yacare*, we use this axis ($Z_{\text{micro:No } yacare}$) to describe the principal axis of morphological differentiation at the intra-specific level when *C. yacare* is excluded from the analyses.

Comparing between $Z_{\text{micro:No } yacare}$ and Z_{macro} showed the angle between the two axes to again be very low (45.1°), and to differ significantly from 90° (Figure S1-c; 73.0° using only *C. crocodilus* subspecies). These results are very similar to the results in the main text when *C. yacare* was included in the analyses, and demonstrate that the nature of cranial shape variation among crocodilians at the interspecific level is highly similar to variation among taxonomic groups within *C. crocodilus* subspecies even when *C. yacare* is excluded from the analysis. Projecting the average shapes for taxonomic groups within *C. crocodilus* but exclusive of *C. yacare* onto the interspecific divergence vector revealed again that the intraspecific groups exhibit a large range of shape variation, spanning the average skull shapes for 10 out of 21 other species of extant crocodilians (Fig. S1-d).

References

Legendre, P. and Legendre, L. 1998. Numerical ecology, volume 20. Elsevier Science.

Pearcy, A. and Wijtten, Z. 2011. A morphometric analysis of crocodilian skull shapes. *The Herpetological Journal* 21:213–218.

Tables

Table S1. Results of multivariate analysis of covariance (MANCOVA) assessing the effects of explanatory variables for cranial shape variation within *Caiman crocodilus*, exclusive of *Caiman yacare*. The MANCOVA is based on fitting linear models where shape variables (relative warps) served as response variables and taxonomic group, centroid size and their interaction served as explanatory variables. Statistical significance for the F tests are based on Wilks's Λ. Although our residuals were not normally distributed when *C. yacare* is removed from the analyses, permutation tests of the F statistics associated with all three terms of the MANCOVA indicated the observed F-statistics to be significantly larger than would be expected by chance.

Explanatory term	F	$d.f$	P	η^2
Centroid size (CS)	6.73	12, 43	0.0034	65.25
Taxonomic group (TG)	3.12	36, 127.8	< 0.0001	46.30
CS $\times$ TG	2.49	36, 127.8	< 0.0001	40.71

Figures

Figure S1-a. The distribution of cranial shape as a function of centroid size in *Caiman crocodilus*. Larger individuals have a more longirostrine cranial shape than smaller individuals The vertical axis describes the shape scores obtained from regressing relative warp scores against taxonomic group and centroid size (see text for details). The predicted landmark coordinates of the largest and smallest *C. crocodilus* individuals were then mapped along with thin-plate-spline deformation grids to illustrate the shape changes relative to the average predicted shape. In this, as in Figures 2 and 3 of the main text, crosses represent *C. crocodilus apaporiensis* individuals, filled grey circles represent *C. crocodilus crocodilus* individuals, asterisks represent *C. crocodilus chiapasius* individuals and open circles represent *C. crocodilus fuscus*.

Figure S1-b. Cranial shape differentiation across taxonomic groups within *C. crocodilus* controlling for the effects of allometry. Here we plot the scores for the first divergence vector associated with the taxonomic group term from the MANCOVA describing shape variation across taxonomic groups with data from subspecies of *C. crocodilus*, excluding *C. yacare*. The horizontal axis represents the primary manner in which taxonomic groups differ in cranial shape, controlling for allometric variation. Cranial shape differences are shown with thin-plate spline transformation grids of the predicted shape relative to the mean set of landmarks.

Figure S1-c. The bootstrapped distribution (from 10,000 iterations) of the angles between Z_{macro} and $Z_{\text{micro:No } yacare}$.

Figure S1-d. Occupation along Z_{macro}, the first PC of the non-allometric component of the relative warps for the interspecific dataset derived from Pearcy and Wijtten (2011) (cross marks on solid, grey line). The data point for the mean *Caiman crocodilus* skull from Pearcy and Wijtten (2011) (open square, grey line) was projected *a posteriori* onto the axis derived from the interspecific dataset *Caiman crocodilus* excluded. Average skull shape for each taxonomic group within *Caiman crocodilus*, exclusive of *Caiman yacare* (black dots on dashed line) were projected onto this axis to permit the comparison of the non-allometric component of shape variation in both groups along a common axis. The abbreviations used for the inter-specific data points are the same as Figure 4a in the main text.

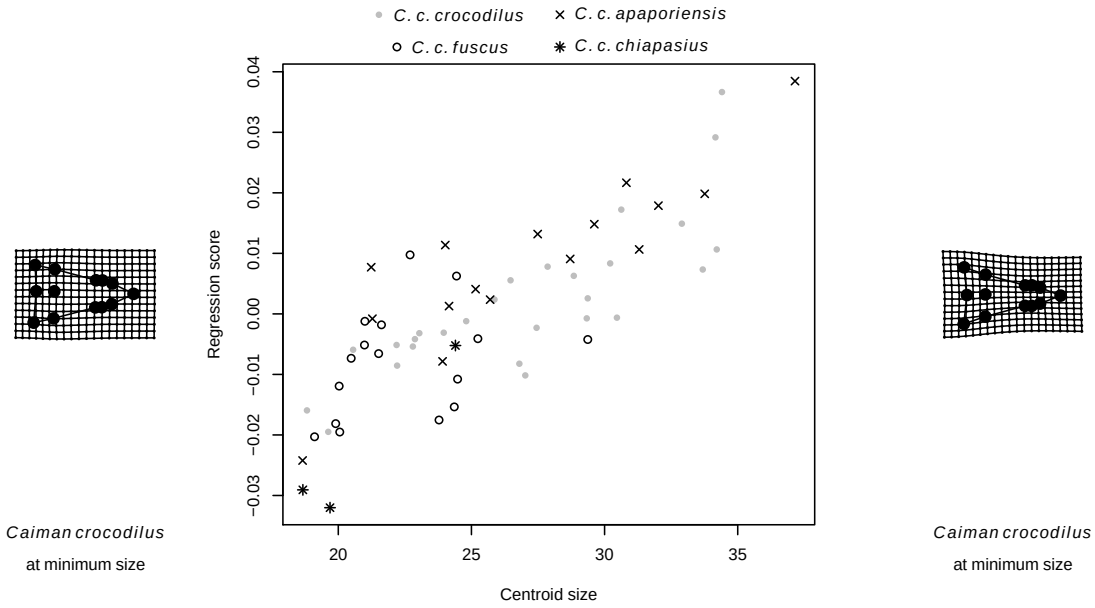
C. c. crocodilus
C. c. apaporiensis
C. c. fuscus
C. c. chiapasius
Regression score
0.04
0.03
0.02
0.01
0.00
−0.01
−0.02
−0.03
20
25
30
35
Centroid size
Caiman crocodilus
at minimum size
Caiman crocodilus
at minimum size

S1-a

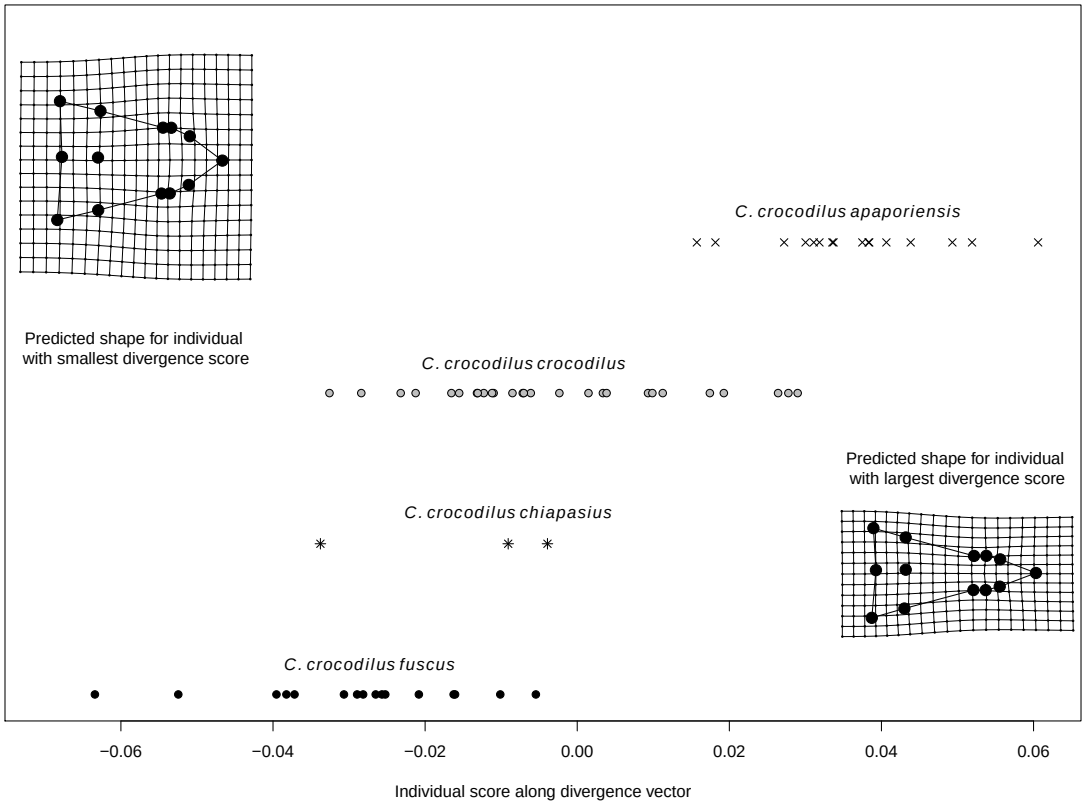
Predicted shape for individual
with smallest divergence score
C. crocodilus apaporiensis
C. crocodilus crocodilus
Predicted shape for individual
with largest divergence score
C. crocodilus chiapasius
C. crocodilus fuscus
−0.06
−0.04
−0.02
0.00
0.02
0.04
0.06
Individual score along divergence vector

S1-b

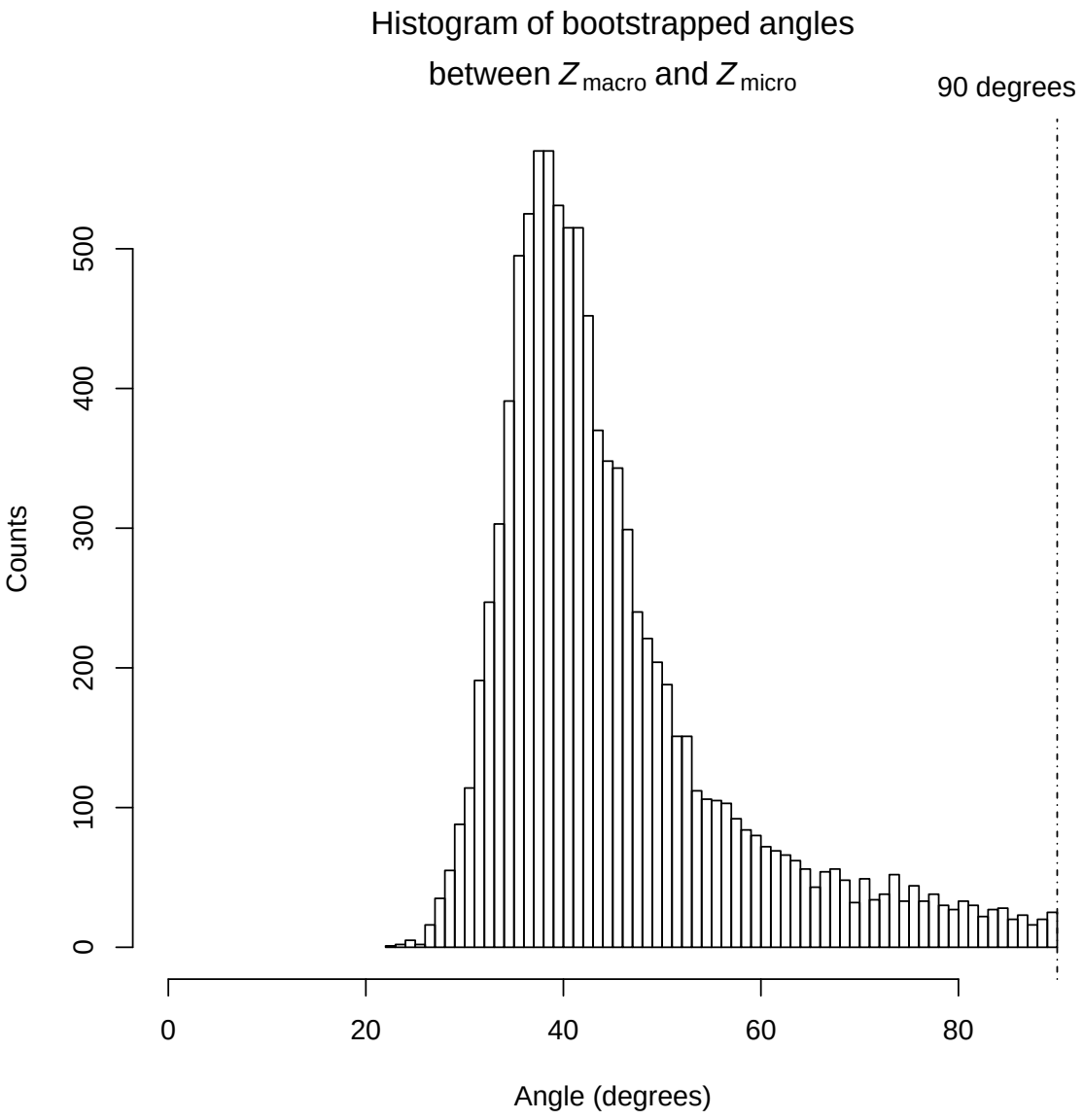
Histogram of bootstrapped angles
between Z_{macro} and Z_{micro}
90 degrees
Counts
0
100
200
300
400
500
0
20
40
60
80
Angle (degrees)

S1-c

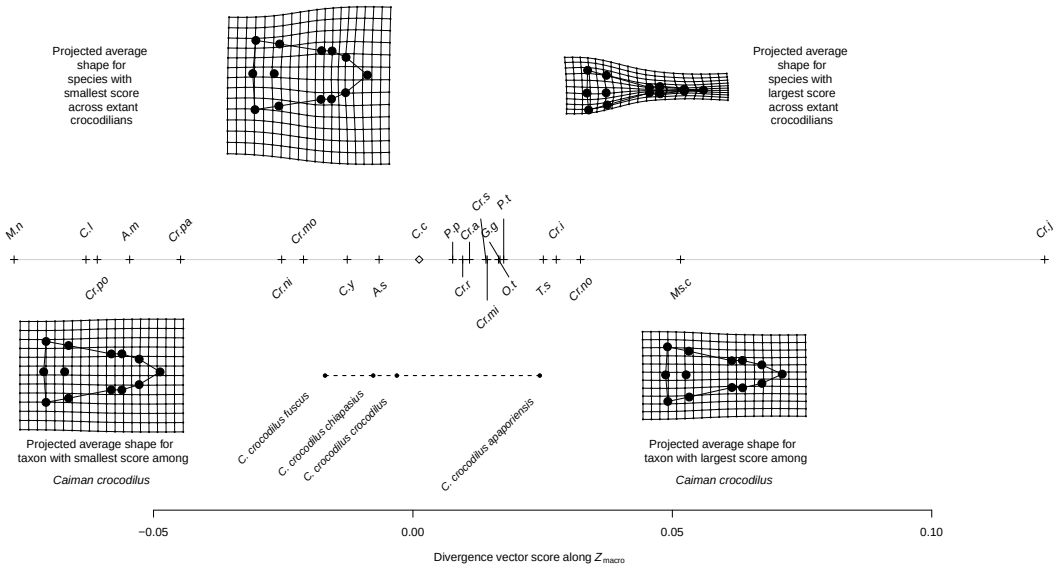
Projected average shape for species with smallest score across extant crocodilians
Projected average shape for species with largest score across extant crocodilians
M.n
C.l
A.m
Cr.pa
Cr.mo
C.c
P.p
Cr.a
S.g
Cr.s
P.t
Cr.i
Cr.j
Cr.po
Cr.ni
C.y
A.s
Cr.r
Cr.mi
O.t
T.s
Cr.no
Ms.c
Projected average shape for taxon with smallest score among Caiman crocodilus
C. crocodilus fuscus
C. crocodilus chiapasius
C. crocodilus crocodilus
C. crocodilus apaporiensis
Projected average shape for taxon with largest score among Caiman crocodilus
−0.05
0.00
0.05
0.10
Divergence vector score along Z_{macro}

S1-d

Supplementary Information S2: Catalog ID (or relevant figure from Medem 1983) and details of specimens used in analysis

Specimen ID	Taxon	Cranial length (cm)	Sex, if known	Geographic origin, if known
FLMNH39062	*Caiman crocodilus crocodilus*	28.7	-	Barinas, Venezuela
DGM*300-RR	*Caiman crocodilus crocodilus*	22.1	-	Acre, Brazil
LACM162652	*Caiman crocodilus crocodilus*	32.6	-	Monagas, Venezuela
AMNH43291	*Caiman crocodilus crocodilus*	24.2	-	Bolívar, Venezuela
FLMNH80910	*Caiman crocodilus crocodilus*	21.7	Female	Guárico, Venezuela
FLMNH80911	*Caiman crocodilus crocodilus*	20.4	Female	Guárico, Venezuela
FLMNH80916	*Caiman crocodilus crocodilus*	22.0	-	Guárico, Venezuela
FLMNH80924	*Caiman crocodilus crocodilus*	18.1	Male	Guárico, Venezuela
FLMNH80930	*Caiman crocodilus crocodilus*	15.9	Female	Guárico, Venezuela
FLMNH80933	*Caiman crocodilus crocodilus*	20.7	Female	Guárico, Venezuela
FLMNH80935	*Caiman crocodilus crocodilus*	26.6	Male	Guárico, Venezuela
FLMNH80936	*Caiman crocodilus crocodilus*	30.9	Male	Guárico, Venezuela
FLMNH80938	*Caiman crocodilus crocodilus*	20.8	-	Cojedes, Venezuela
FLMNH80949	*Caiman crocodilus crocodilus*	15.1	Female	Guárico, Venezuela
MedemFig20	*Caiman crocodilus crocodilus*	29.2	Male	Boyacá, Colombia
MedemFig23	*Caiman crocodilus crocodilus*	28.4	Male	Vichada, Colombia
MedemFig24	*Caiman crocodilus crocodilus*	31.2	Male	Guainia, Colombia
MedemFig21	*Caiman crocodilus crocodilus*	25.6	Male	Casanare, Colombia
MedemFig22	*Caiman crocodilus crocodilus*	26.1	Male	Meta, Colombia
MedemFig28	*Caiman crocodilus crocodilus*	29.0	Male	Caquetá, Colombia
MedemFig25	*Caiman crocodilus crocodilus*	28.1	Male	Vaupés, Colombia
MedemFig29	*Caiman crocodilus crocodilus*	32.5	Male	Putumayo, Colombia
MedemFig30	*Caiman crocodilus crocodilus*	27.7	Male	Amazonas, Colombia
USNM134499	*Caiman crocodilus apaporiensis*	25.6	-	Amazonas, Colombia
FMNH69832	*Caiman crocodilus apaporiensis*	19.9	-	Amazonas, Colombia
FMNH69825	*Caiman crocodilus apaporiensis*	18.4	-	Amazonas, Colombia
FMNH69831	*Caiman crocodilus apaporiensis*	32.0	-	Amazonas, Colombia
FMNH69821	*Caiman crocodilus apaporiensis*	28.9	-	Amazonas, Colombia
FMNH69820	*Caiman crocodilus apaporiensis*	24.6	-	Amazonas, Colombia
FMNH69814	*Caiman crocodilus apaporiensis*	24.5	-	Amazonas, Colombia
FMNH69828	*Caiman crocodilus apaporiensis*	25.5	-	Amazonas, Colombia
FMNH69812	*Caiman crocodilus apaporiensis*	33.2	-	Amazonas, Colombia
FMNH69816	*Caiman crocodilus apaporiensis*	24.0	-	Amazonas, Colombia
FMNH69813	*Caiman crocodilus apaporiensis*	28.9	-	Amazonas, Colombia
FMNH69826	*Caiman crocodilus apaporiensis*	27.5	-	Amazonas, Colombia
FMNH69830	*Caiman crocodilus apaporiensis*	30.2	-	Amazonas, Colombia
FMNH69824	*Caiman crocodilus apaporiensis*	19.9	-	Amazonas, Colombia
MedemFig27	*Caiman crocodilus apaporiensis*	23.5	Female	Meta, Colombia
MedemFig26	*Caiman crocodilus apaporiensis*	29.0	Male	Vaupés, Colombia
SMF43953	*Caiman crocodilus apaporiensis*	22.2	Female	Amazonas, Colombia
USNM115336	*Caiman crocodilus chiapasius*	21.9	-	Chiapas, Mexico
USNM115334	*Caiman crocodilus chiapasius*	29.5	-	Chiapas, Mexico

*Divisão de Geologia e Minerologia, Brazil

Specimen ID	Taxon	Cranial length (cm)	Sex, if known	Geographic origin, if known
USNM115335	*Caiman crocodilus chiapasius*	21.7	-	Chiapas, Mexico
MedemFig18	*Caiman crocodilus fuscus*	19.4	Male	Chocó, Colombia
MedemFig19	*Caiman crocodilus fuscus*	19.3	Male	Cauca, Colombia
FLMNH80942	*Caiman crocodilus fuscus*	17.3	Female	Zulia, Venezuela
FMNH69862	*Caiman crocodilus fuscus*	22.6	-	Magdalena, Colombia
FMNH69844	*Caiman crocodilus fuscus*	19.2	-	Magdalena, Colombia
FMNH69842	*Caiman crocodilus fuscus*	22.4	-	Magdalena, Colombia
FMNH69852	*Caiman crocodilus fuscus*	22.5	-	Magdalena, Colombia
FMNH69858	*Caiman crocodilus fuscus*	19.8	-	Magdalena, Colombia
FMNH69849	*Caiman crocodilus fuscus*	22.8	-	Magdalena, Colombia
USNM65841	*Caiman crocodilus fuscus*	28.3	-	Panama Canal Zone, Panama
USNM65843	*Caiman crocodilus fuscus*	28.0	-	Panama Canal Zone, Panama
USNM102718	*Caiman crocodilus fuscus*	26.2	-	Panama Canal Zone, Panama
USNM313860	*Caiman crocodilus fuscus*	23.9	-	Bocas del Toro, Panama
USNM313866	*Caiman crocodilus fuscus*	22.5	-	Panama Canal Zone, Panama
MedemFig15	*Caiman crocodilus fuscus*	28.1	Male	Córdoba, Colombia
MedemFig17	*Caiman crocodilus fuscus*	18.7	Female	Córdoba, Colombia
AMNH120028	*Caiman yacare*	22.1	-	-
FLMNH121249	*Caiman yacare*	34.5	-	Alto Paraguay, Paraguay
FLMNH121263	*Caiman yacare*	28.5	-	Alto Paraguay, Paraguay
USNM281806	*Caiman yacare*	31.0	-	Beni, Bolivia
USNM281808	*Caiman yacare*	32.5	-	Beni, Bolivia
USNM281810	*Caiman yacare*	31.1	-	Beni, Bolivia
USNM281811	*Caiman yacare*	23.2	-	Beni, Bolivia
USNM281814	*Caiman yacare*	24.5	-	Beni, Bolivia
USNM281816	*Caiman yacare*	19.5	-	Beni, Bolivia
USNM281821	*Caiman yacare*	29.8	-	Beni, Bolivia
USNM281824	*Caiman yacare*	23.0	-	Beni, Bolivia
USNM281829	*Caiman yacare*	28.8	-	Beni, Bolivia
USNM281830	*Caiman yacare*	21.9	-	Beni, Bolivia
USNM281834	*Caiman yacare*	29.6	-	Beni, Bolivia
USNM281835	*Caiman yacare*	31.9	-	Beni, Bolivia
USNM281836	*Caiman yacare*	26.9	-	Beni, Bolivia
USNM281837	*Caiman yacare*	31.3	-	Beni, Bolivia
USNM281839	*Caiman yacare*	31.0	-	Beni, Bolivia
USNM281840	*Caiman yacare*	28.7	-	Beni, Bolivia
USNM281846	*Caiman yacare*	23.2	-	Beni, Bolivia
USNM281848	*Caiman yacare*	33.4	-	Beni, Bolivia
AMNH97299	*Caiman yacare*	19.5	-	Beni, Bolivia
AMNH97300	*Caiman yacare*	33.3	-	Beni, Bolivia
AMNH97303	*Caiman yacare*	19.7	-	Beni, Bolivia
AMNH97309	*Caiman yacare*	24.6	-	Beni, Bolivia
AMNH97329	*Caiman yacare*	26.0	-	Beni, Bolivia
AMNH97330	*Caiman yacare*	26.8	-	Beni, Bolivia
AMNH97331	*Caiman yacare*	21.0	-	Beni, Bolivia
FMNH9145	*Caiman yacare*	27.9	-	Brazil
FMNH9147	*Caiman yacare*	23.2	-	Brazil
FMNH9144	*Caiman yacare*	31.7	-	Brazil
FMNH9136	*Caiman yacare*	35.6	-	Brazil
FMNH9143	*Caiman yacare*	36.0	-	Brazil
SMFNO6	*Caiman yacare*	19.4	-	Corrientes, Argentina
SMF30107	*Caiman yacare*	29.1	-	Argentina

References

Medem, F. 1983. Los Crocodylia de Sur America Volumen II. Ministerio de Educación Nacional, Bogotá, Colombia.

Supplementary Information S3

Statistical analyses of the effects of approximate life stage and sex

Approximate Life Stage

Caiman crocodilus individuals are believed to mature by the time they exceed 140 cm in total length (Holmback 1981); based on the measurements of total length and cranial length reported in Medem 1983, all individuals with total cranial lengths greater than 20 cm had total lengths greater than 140 cm. Thus, we characterized individuals with cranial lengths smaller than 20 cm as subadults, and analyzed whether differences in cranial shape was associated with the specimen's life stage (mature adult or subadult), controlling for body size. Fitting a linear model of the form:

Relative warps = constant + Life Stage + Centroid Size + Error, (S3-a)

we found no evidence for different cranial shapes between adult and sub-adult individuals either with *C. yacare* (Wilks' Λ =0.84, F=1.22, d.f=12,79, p = 0.29 for life stage; Wilks' Λ =0.62, F=4.03, d.f=12,79, p < 0.001 for centroid size; n=93) or without *C. yacare* (Wilks' Λ =0.70, F=1.75, d.f=12,48, p = 0.085 for life stage; Wilks' Λ =0.38, F=6.54, d.f=12,48, p < 0.0001 for centroid size; n=62).

Sex

Of the 62 *C. crocodilus* specimens used in the analysis, data on the sex of the individuals were available for a subset (n=28) of the specimens. We assessed whether sexual dimorphism in cranial shape was observable among these individuals by conducting a separate MANCOVA that involved regressing the shape variables against an additive effect for both sex and body size. Fitting a linear model of the form:

Relative warps = constant + Sex + Centroid size + Error (S3-b)

where the subscript s denotes the fact that this analysis is based on a subset of our total data set. Within this data subset, we found no evidence for sexual dimorphism in cranial shape (Wilks' Λ =0.51, F=1.12,

d.f=12,14, p = 0.42 for sex; Wilks' Λ =0.19, F=5.11, d.f=12,14, p = 0.0025 for centroid size; $n_{females}$ = 10, n_{males} = 18).

References:

HOLMBACK, E. 1981. Reproduction of the brown caiman *Caiman crocodilus fuscus* at the San Antonio Zoo. *Int Zoo Yearb* 21:77–79.

MEDEM, F. 1983. Los Crocodylia de Sur America Volumen II. Ministerio de Educación Nacional, Bogotá, Colombia.

Supplementary Information S4 - Discriminating *Caiman crocodilus apaporiensis* and *Caiman yacare* specimens

Our study included a modest (N=16) sample of *C. c. apaporiensis* specimens, providing us with an opportunity to assess whether using a quantitative characterization of cranial shape in *C. c. apaporiensis* can reliably classify individual specimens as belonging to *C. c. apaporiensis* based on the principal components of our landmarks. Specifically, we used a combination of the naive Bayes classifier (Mitchell 1997) and leave-one-out cross validation to assess the frequency with which individual specimens are accurately classified as either *C. c. apaporiensis* or not. Briefly, if observation i is associated with measurements $X_{1_i}, X_{2_i}, ...$ (e.g., the value of principal component 1 for specimen i, the value of principal component 2 for specimen i, etc...) and a discrete class C (e.g., subspecies), the naive Bayes classifier assigns an observation i to class C that maximizes the conditional probability of observing $X_{1_i}, X_{2_i}, ...$ given that i belongs to class C (Mitchell 1997). For each specimen, we can construct a naive Bayes classifier relating the principal component axes to the different subspecies using all other specimens as a training data set. We can then use the naive Bayes classifier to assign a subspecies to the omitted specimen, and assess whether the subspecies designation of *C. c. apaporiensis* predicted by the naive Bayes classifier was accurate. Using the same approach, we also sought to analyze the extent to which the cranial shapes of *C. yacare* quantitatively differ from the cranial shapes of *C. crocodilus*. Uncertainty in the ability of the naive Bayes classifiers to predict the subspecies desgination was assessed by resampling from the data and repeating the analysis (n=5000). To implement this analysis, we used the naive Bayes classifiers from the package e1071 in R (Dimitriadou et al. 2011).

We find that when the training data excluded *C. yacare* specimens, the naive Bayes classifier based on the first two principal component axes could correctly classify an average of 81.6% of *C. crocodilus apaporiensis* specimens included from the training data (standard deviation = 10.0%; Figure s4-A); when the naive Bayes classifier was trained on a data set that excluded *C. yacare*, the average percentage of correct assignment to *C. crocodilus apaporiensis* was 87.5% ($\pm$ 8.4 %); Figure S4-B). The naive Bayes classifier was able to distinguish *C. yacare* at a higher rate (average percentage of correct assignment $\approx$ 90.3% ($\pm$ 5.4 %); Figure S4-C).

Figure captions

Supplementary Figure S6. Histograms of resampled runs for the leave-one-out cross validated naive-bayes classifier for assigning the specimen excluded from the training data to the correct taxon based on the first two PC axes. (A) *C. c. apaporiensis* specimens when the training data included *C. yacare*, (B) *C. c. apaporiensis* specimens when the training data excluded *C. yacare*, and (C) *C. yacare* specimens when other *C. yacare* specimens were included in the training data. The first two PCs were reliably able to assign specimens excluded from the training data to *C. c. apaporiensis* whether *C. yacare* was included in the training data or not. The same PCs were unable to correctly assign all *C. yacare* specimens consistently, resulting in a less-skewed distribution of the classfier's performance.

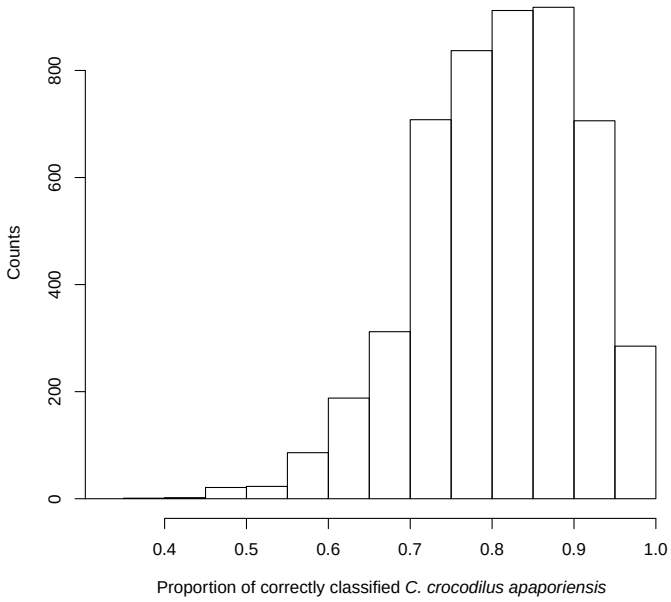

(A)

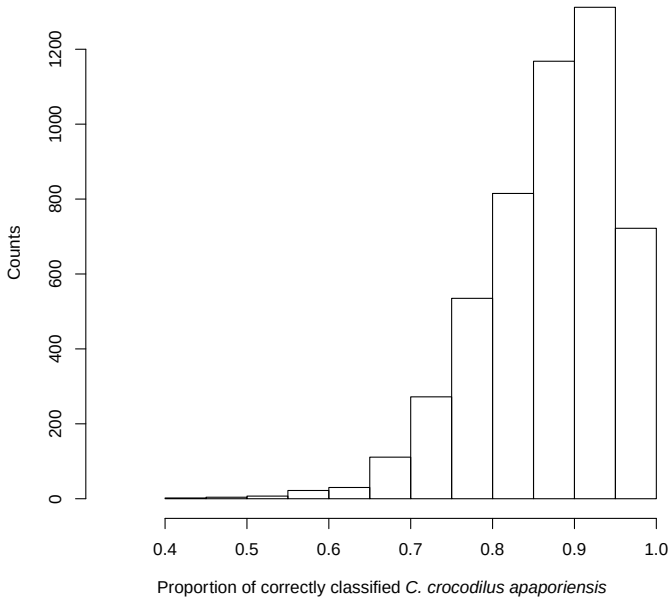

(B)

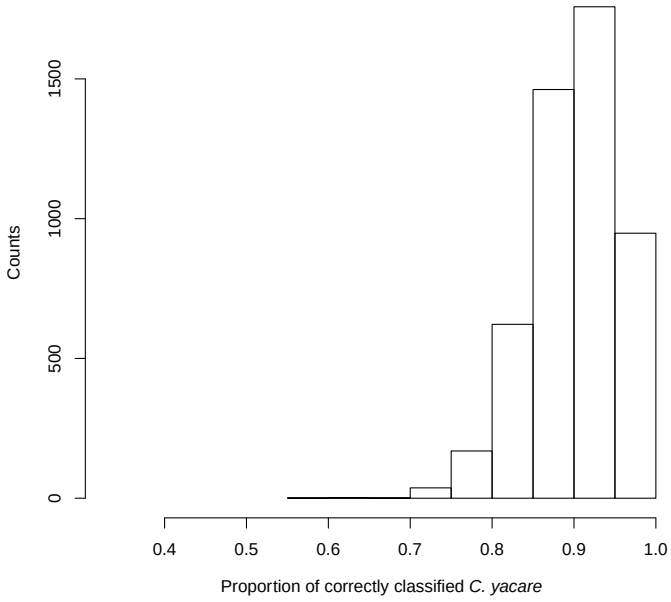

(C)

Figure s4

1

References

Dimitriadou, E., Hornik, K., Leisch, F., Meyer, D., and Weingessel, A. 2011. e1071: Misc Functions of the Department of Statistics (e1071), TU Wien.

Mitchell, T. 1997. Machine Learning. McGraw Hill.